ELSEVIER

Engineering Analysis with Boundary Elements 28 (2004) 1493–1513

ENGINEERING ANALYSIS *with* BOUNDARY ELEMENTS

www.elsevier.com/locate/enganabound

A weakly singular boundary integral equation in elastodynamics for heterogeneous domains mitigating fictitious eigenfrequencies

Lincy Pyl[a,*], Didier Clouteau[b], Geert Degrande[a]

[a]*Department of Civil Engineering, K.U. Leuven, Kasteelpark Arenberg 40, B-3001 Leuven, Belgium*
[b]*LMSSMat, Ecole Centrale de Paris, Grande Voie des Vignes, F-92295 Châtenay Malabry, France*

Abstract

A boundary element formulation applied to dynamic soil–structure interaction problems with embedded foundations may give rise to inaccurate results at frequencies that correspond to the eigenfrequencies of the finite domain embedded in an exterior domain of semi-infinite extent. These frequencies are referred to as fictitious eigenfrequencies. This problem is illustrated and mitigated modifying the original approach proposed by Burton and Miller for acoustic problems, which combines the boundary integral equations in terms of the displacement and its normal derivative using a complex coupling parameter α. Hypersingular terms in the original boundary integral equation are avoided by replacing the normal derivative by a finite difference approximation over a characteristic distance h, still leading to an exact boundary integral equation. A proof of the uniqueness of this formulation for small h and a smooth boundary is given, together with a parametric study for the case of a rigid massless cylindrical embedded foundation. General conclusions are drawn for the practical choice of the dimensionless coupling parameter $\bar{\alpha}$ and the dimensionless distance $\bar{h}$.

Keywords: Boundary integral equation; Elastodynamics; Fictitious eigenfrequencies; Dynamic soil–structure interaction

1. Introduction

The response of a structure to external forces, a seismic excitation or traffic induced vibrations can be calculated using a subdomain formulation for dynamic soil–structure interaction [1,2]. The structure may have a surface or embedded foundation and is usually modeled with the finite element method (FEM), while a boundary element method (BEM) is generally preferred to model the soil domain of semi-infinite extent. If the boundary element formulation is based on the Green's functions for a horizontally layered halfspace [3–7], only a discretization of the interface between the soil and the structure is required and the number of unknowns is drastically reduced.

The solution for the unbounded soil domain is not straightforward, however, as any displacement boundary integral equation, regularized or not, that is used to derive the boundary element formulation has a non-unique solution at frequencies corresponding to the eigenfrequencies of the excavated part of the soil with Dirichlet boundary conditions on the interface between the soil and the foundation, and free surface conditions elsewhere [8–10]. For structures embedded in a semi-infinite halfspace, this numerical deficiency predominantly occurs in the high frequency range, depending on the geometry of the foundation and the stiffness of the excavated soil. Therefore, the problem of fictitious frequencies is not very stringent for applications in seismic engineering, where the excitation frequencies are low (typically between 0 and 10 Hz). For applications of traffic induced vibrations, however, the excitation frequencies are an order of magnitude higher (between 1 and 80 Hz) and fictitious frequencies need to be mitigated, which is the motivation of the present work.

A similar phenomenon is well known in acoustics, where the problem of fictitious eigenfrequencies has been studied extensively. Several solution techniques have been proposed in the literature and are summarized below.

Copley [11] was the first to report a solution method, using the second or interior Helmholtz integral equation and enforcing zero displacements in the interior domain.

* Corresponding author. Tel.: +32 16 32 16 75; fax: +32 16 32 19 88.
E-mail address: lincy.pyl@bwk.kuleuven.ac.be (L. Pyl).

0955-7997/$ - see front matter © 2004 Elsevier Ltd. All rights reserved.
doi:10.1016/j.enganabound.2004.08.001

Schenck [12] developed the CHIEF method, using the combined surface and interior Helmholtz integral equations. Zero displacements are enforced at discrete points in the interior domain, resulting in an overdetermined system of equations, that is solved with a least squares procedure. A similar approach is used by Piaszczyk [13].

An effective and widely used method to mitigate fictitious frequencies has been proposed by Burton and Miller [14] and consists of writing a linear combination of the original boundary integral equation for the pressure and its normal derivative. Both integral equations have a non-unique solution at frequencies corresponding to the eigenfrequencies of an interior Dirichlet or Neumann problem, respectively. A unique solution is obtained provided that the coupling parameter linking these boundary integral equations has a non-zero imaginary part. The choice of this coupling parameter is not critical and a small imaginary number is sufficient to mitigate the problem of the fictitious eigenfrequencies. Amini [15] has shown that, for a spherical cavity in an acoustic problem, the lowest condition number of the integral operators in Burton and Miller's formulation is obtained when the coupling parameter is inversely proportional to the wave number k_p of the longitudinal wave. A drawback of Burton and Miller's method in the context of elastodynamics is that strongly singular kernels are introduced through the boundary integral equation for the traction. For acoustic problems, Burton and Miller review several methods to transform these integral operators [14].

Chen et al. [16,17] have also used the dual BEM for 2D exterior acoustic problems in combination with Burton and Miller's method. They introduced the concept of modal participation factors to elucidate the appearance of fictitious frequencies related to the singular and hypersingular boundary integral equations. The four kernels in the integral equations, as well as the boundary potential and the flux, are expanded in Fourier series along the circumferential direction, while Bessel functions are used in the radial direction. Using these expansions, the singular boundary integral equation for the exterior domain is expressed for points located outside the exterior domain of interest. The resulting boundary potential is written as a Fourier series expansion on the circumferential modes. The coefficients in this expression are written as the product of a modal participation factor and a factor revealing numerical instability at fictitious eigenfrequencies. A similar analysis prevails for the hypersingular integral equation. These concepts are illustrated for several 2D acoustic radiation and scattering problems. Numerical results obtained with the dual BEM are compared with analytical results and numerical results computed with Burton and Miller's method, Schenck's method and the DtN method.

Ursell [18] and Jones [19] describe a new fundamental solution that is equal to zero in the interior domain. Brod [20] uses the same technique and demonstrates that an infinite set of integral equations on the boundary, using a series expansion of the Green's function, has a unique solution for all wave numbers.

Kobayashi and Nishimura [21] extended Jones' method to elastodynamic problems, using a modified fundamental solution that satisfies a boundary integral equation for the exterior Neumann problem. For the dynamic analysis of underground structures, Kobayashi and Nishimura interpolate the solution obtained at frequencies that are slightly lower and higher than the fictitious eigenfrequencies [22,23].

Gonsalves et al. [24] proposed a numerical solution procedure for 3D elastodynamic transmission problems using a system of coupled boundary integral equations and the combination of the surface and interior Helmholtz integral equation introduced by Schenck to overcome the non-uniqueness of the boundary integral equation solution at the fictitious eigenfrequencies.

Jones modified Burton and Miller's method for applications in elastodynamics [25]. As some of the integrals are highly singular, a numerical technique using a boundary discretization with constant elements is introduced.

Liu and Rizzo [26] first demonstrated the effectiveness of the weakly singular form of the hypersingular boundary integral equation using the static Kelvin solution as a fundamental solution. The boundary discretization is not limited to flat elements, contrary to Jones' regularization technique. A traction-free spherical void excited by a P-wave of unit amplitude, using Overhauser C^1 continuous elements and non-conforming quadratic elements, is investigated. Good results are obtained if an imaginary coupling coefficient is used that is inversely proportional to the wave number k_p of the longitudinal wave. Alternatively, the wave number k_s of the shear wave could have been chosen.

The first objective of this paper is to briefly review the subdomain formulation for the solution of dynamic soil–structure interaction problems. The impedance of the soil and the force due to the incident wave field are calculated with a BEM using the Green's functions of a layered halfspace. Next, the problem of fictitious eigenfrequencies associated with the displacement boundary integral equation for exterior domains is recalled. Burton and Miller's solution method, that has been extended to elastodynamic problems by Jones [25] and Liu and Rizzo [26], is modified to mitigate the problem. In order to obtain a well-posed boundary integral equation at all frequencies, a linear combination of the boundary integral equation for the displacement and for the displacement gradient along the normal direction of the boundary is made, using a complex coupling parameter α. This corresponds to a mixed boundary condition on the interior domain. Hypersingular terms in the resulting boundary integral equation are avoided by replacing the normal derivative by a finite difference approximation over a characteristic distance h, still leading to an exact boundary integral equation. A parametric study is finally performed for the case of

a rigid massless cylindrical embedded foundation. General conclusions are drawn for a practical choice of the dimensionless coupling parameter $\bar{\alpha}$ and the dimensionless distance $\bar{h}$.

2. The numerical prediction model

This section reviews the subdomain formulation for dynamic soil–structure interaction problems [1,2] that are formulated to assess traffic induced vibrations in the built environment. This allows to demonstrate the role of the soil impedance and the force vector due to an incident wave in the governing system of equations, which are calculated with a boundary element formulation. For structures with an embedded foundation, the boundary integral equation leads to fictitious eigenfrequencies corresponding to the eigenfrequencies of the excavated part of the soil.

The problem is decomposed into two subdomains (Fig. A.1): the structure Ω_b and the exterior soil domain Ω_s^{ext} (Fig. A.2b) after excavation of the interior soil domain Ω_s^{int} (Fig. A.2c). The semi-infinite layered soil domain Ω_s prior to excavation is denoted by $\Omega_s = \Omega_s^{\text{ext}} \cup \Omega_s^{\text{int}}$ (Fig. A.2a). The problem is solved by enforcing continuity of displacements and equilibrium of stresses on the interface Σ between both subdomains. In the following, linear problems will be assumed and all equations will be elaborated in the frequency domain.

First, the structure Ω_b is considered. The boundary $\Gamma_b = \Gamma_{b\sigma} \cup \Sigma$ of the structure Ω_b is decomposed into a boundary $\Gamma_{b\sigma}$ where tractions $\bar{\mathbf{t}}_b$ are imposed and the soil–structure interface Σ. The displacement vector $\mathbf{u}_b$ of the structure satisfies the following Navier equation and boundary conditions:

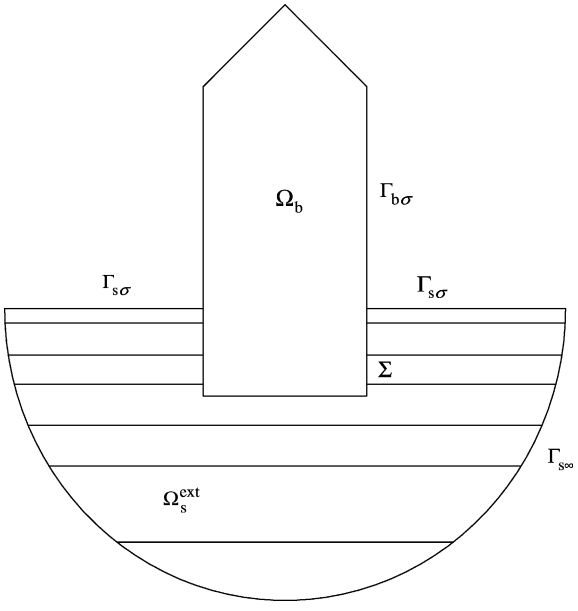

Fig. A.1. Geometry of the subdomains.

$$\operatorname{div} \boldsymbol{\sigma}_b(\mathbf{u}_b) + \rho_b \mathbf{b} = -\rho_b \omega^2 \mathbf{u}_b \quad \text{in } \Omega_b \tag{1}$$

$$\mathbf{t}_b(\mathbf{u}_b) = \bar{\mathbf{t}}_b \quad \text{on} \quad \Gamma_{b\sigma} \tag{2}$$

$$\mathbf{u}_b = \mathbf{u}_s \quad \text{on } \Sigma \tag{3}$$

$$\mathbf{t}_b(\mathbf{u}_b) + \mathbf{t}_s(\mathbf{u}_s) = 0 \quad \text{on } \Sigma \tag{4}$$

where $\rho_b \mathbf{b}$ denotes the body force on the structure and $\mathbf{t}(\mathbf{u}) = \boldsymbol{\sigma}(\mathbf{u}) \cdot \mathbf{n}$ the traction vector on a boundary with a unit outward normal vector $\mathbf{n}$. In Eqs. (3) and (4), displacement continuity and stress equilibrium are imposed on the interface Σ. $\mathbf{u}_s$ denotes the displacement vector in the soil. Using modal decomposition, the structural displacement vector $\mathbf{u}_b$ is expanded with bounded error on a finite basis of modes $\boldsymbol{\psi}_m$ ($m = 1,\ldots,q$):

$$\mathbf{u}_b = \sum_{m=1}^{q} \boldsymbol{\psi}_m \alpha_m \quad \text{in } \Omega_b \tag{5}$$

where the modal coordinates α_m ($m = 1,\ldots,q$) will be collected in a vector $\boldsymbol{\alpha}$.

Secondly, the exterior soil domain Ω_s^{ext} is taken into consideration. The boundary $\Gamma_s^{\text{ext}} = \Gamma_{s\sigma} \cup \Gamma_{s\infty} \cup \Sigma$ of the soil domain Ω_s^{ext} is decomposed into the boundary $\Gamma_{s\sigma}$ where tractions are imposed, the outer boundary $\Gamma_{s\infty}$ on which radiation conditions are imposed and the soil–structure interface Σ. A free boundary or zero tractions are assumed on $\Gamma_{s\sigma}$ in the following. The displacement vector $\mathbf{u}_s$ of the soil satisfies the Navier equation and the following boundary conditions:

$$\operatorname{div} \boldsymbol{\sigma}_s(\mathbf{u}_s) + \rho_s \mathbf{b} = -\rho_s \omega^2 \mathbf{u}_s \quad \text{in} \quad \Omega_s^{\text{ext}} \tag{6}$$

$$\mathbf{t}_s(\mathbf{u}_s) = 0 \quad \text{on} \quad \Gamma_{s\sigma} \tag{7}$$

$$\mathbf{R}(\mathbf{u}_s) = 0 \quad \text{on} \quad \Gamma_{s\infty} \tag{8}$$

$$\mathbf{u}_s = \mathbf{u}_b \quad \text{on } \Sigma \tag{9}$$

$$\mathbf{t}_b(\mathbf{u}_b) + \mathbf{t}_s(\mathbf{u}_s) = 0 \quad \text{on } \Sigma \tag{10}$$

with $\rho_s \mathbf{b}$ the body force in the soil. The operator $\mathbf{R}$ in Eq. (8) denotes the radiation conditions of elastodynamics [27] on the displacements $\mathbf{u}_s$ on the outer boundary $\Gamma_{s\infty}$ of the unbounded domain Ω_s^{ext}.

The displacement vector $\mathbf{u}_s$ in the soil is decomposed in the incident wave field $\mathbf{u}_i$ and the diffracted wave field $\mathbf{u}_d$ (Fig. A.3). The diffracted wave field $\mathbf{u}_d$ is expanded into a locally diffracted wave field $\mathbf{u}_{d0}$ that is equal to $-\mathbf{u}_i$ on the interface Σ and the wave fields $\mathbf{u}_{dm}$ that are radiated in the soil due to the motion of the interface Σ [1]:

$$\mathbf{u}_s = \mathbf{u}_i + \mathbf{u}_d = \mathbf{u}_i + \mathbf{u}_{d0} + \sum_{m=1}^{q} \mathbf{u}_{dm} \alpha_m \quad \text{in} \quad \Omega_s^{\text{ext}} \tag{11}$$

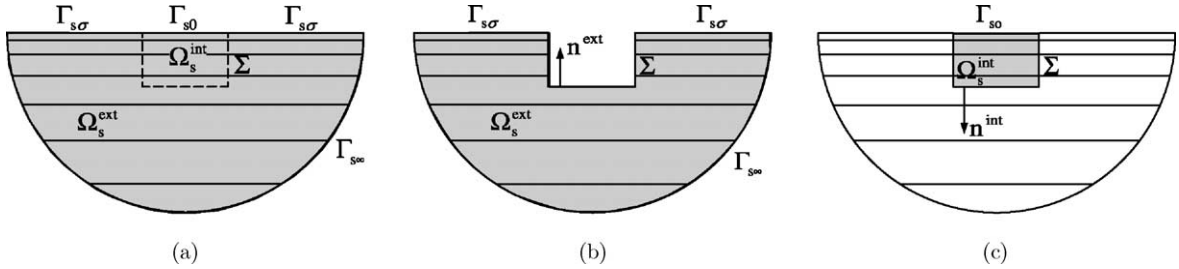

Fig. A.2. (a) The entire and domain $\Omega_s = \Omega_s^{\text{ext}} \cup \Omega_s^{\text{int}}$ before excavation, (b) the exterior soil domain Ω_s^{ext} after excavation, and (c) the interior soil domain Ω_s^{int}.

The incident wave field $\mathbf{u}_i$ is defined on the semi-infinite layered soil domain Ω_s without excavation. The boundary $\Gamma_s = \Gamma_{s0} \cup \Gamma_{s\sigma} \cup \Gamma_{s\infty}$ of the soil domain Ω_s is decomposed into the free surface Γ_{s0} of the excavated part Ω_s^{int} of the soil, the free boundary $\Gamma_{s\sigma}$ and the outer boundary $\Gamma_{s\infty}$. The incident wave field $\mathbf{u}_i$ satisfies the Navier equation and the following boundary condition:

$$\operatorname{div} \boldsymbol{\sigma}_s(\mathbf{u}_i) = -\rho_s \omega^2 \mathbf{u}_i \quad \text{in } \Omega_s \tag{12}$$

$$\mathbf{t}_s(\mathbf{u}_i) = \mathbf{0} \quad \text{on } \Gamma_{s\sigma} \cup \Gamma_{s0} \tag{13}$$

Sommerfeld's radiation conditions on $\Gamma_{s\infty}$ are not satisfied for the incident wave field.

The locally diffracted wave field $\mathbf{u}_{d0}$ is defined on the exterior soil domain Ω_s^{ext} and satisfies the Navier equation and the following boundary conditions:

$$\operatorname{div} \boldsymbol{\sigma}_s(\mathbf{u}_{d0}) = -\rho_s \omega^2 \mathbf{u}_{d0} \quad \text{in } \Omega_s^{\text{ext}} \tag{14}$$

$$\mathbf{t}_s(\mathbf{u}_{d0}) = \mathbf{0} \quad \text{on } \Gamma_{s\sigma} \tag{15}$$

$$\mathbf{R}(\mathbf{u}_{d0}) = \mathbf{0} \quad \text{on } \Gamma_{s\infty} \tag{16}$$

$$\mathbf{u}_{d0} = -\mathbf{u}_i \quad \text{on } \Sigma \tag{17}$$

The displacement fields $\mathbf{u}_{dm}$ radiated in the soil satisfy the following equilibrium equation and boundary conditions:

$$\operatorname{div} \boldsymbol{\sigma}_s(\mathbf{u}_{dm}) = -\rho_s \omega^2 \mathbf{u}_{dm} \quad \text{in } \Omega_s^{\text{ext}} \tag{18}$$

$$\mathbf{t}_s(\mathbf{u}_{dm}) = \mathbf{0} \quad \text{on } \Gamma_{s\sigma} \tag{19}$$

$$\mathbf{R}(\mathbf{u}_{dm}) = \mathbf{0} \quad \text{on } \Gamma_{s\infty} \tag{20}$$

$$\mathbf{u}_{dm} = \boldsymbol{\psi}_m \quad \text{on } \Sigma \tag{21}$$

Eq. (21) expresses continuity of displacements on the soil–structure interface Σ: the displacement field $\mathbf{u}_{dm}$ radiated in the soil is equal to the projection of the structural mode $\boldsymbol{\psi}_m$ $(m=1,\ldots,q)$ on the interface Σ. Every elastodynamic field $\mathbf{u}_{dm}$ creates a traction field $\mathbf{t}_s(\mathbf{u}_{dm})$ on the soil–structure interface Σ, so that the tractions $\mathbf{t}_s(\mathbf{u}_s)$ in the soil are decomposed as follows using Eq. (11):

$$\mathbf{t}_s(\mathbf{u}_s) = \mathbf{t}_s(\mathbf{u}_i + \mathbf{u}_{d0}) + \sum_{m=1}^{q} \mathbf{t}_s(\mathbf{u}_{dm}) \alpha_m \quad \text{on } \Sigma \tag{22}$$

The equilibrium of the structure Ω_b is subsequently expressed in the weak sense for any virtual displacement field $\mathbf{v}$:

$$\int_{\Sigma} \mathbf{v} \cdot \mathbf{t}_b(\mathbf{u}_b)\, \mathrm{d}\Sigma = \int_{\Omega_b} \boldsymbol{\varepsilon}(\mathbf{v}) : \boldsymbol{\sigma}_b(\mathbf{u}_b)\, \mathrm{d}\Omega - \omega^2 \int_{\Omega_b} \mathbf{v} \cdot \rho_b \mathbf{u}_b\, \mathrm{d}\Omega - \int_{\Gamma_{b\sigma}} \mathbf{v} \cdot \bar{\mathbf{t}}_b\, \mathrm{d}\Gamma - \int_{\Omega_b} \mathbf{v} \cdot \rho_b \mathbf{b}\, \mathrm{d}\Omega \tag{23}$$

Accounting for the stress equilibrium (4) on the soil–structure interface Σ, the equilibrium equation (23) becomes:

$$\int_{\Omega_b} \boldsymbol{\varepsilon}(\mathbf{v}) : \boldsymbol{\sigma}_b(\mathbf{u}_b)\, \mathrm{d}\Omega - \omega^2 \int_{\Omega_b} \mathbf{v} \cdot \rho_b \mathbf{u}_b\, \mathrm{d}\Omega + \int_{\Sigma} \mathbf{v} \cdot \mathbf{t}_s(\mathbf{u}_s)\, \mathrm{d}\Sigma = \int_{\Gamma_{b\sigma}} \mathbf{v} \cdot \bar{\mathbf{t}}_b\, \mathrm{d}\Gamma + \int_{\Omega_b} \mathbf{v} \cdot \rho_b \mathbf{b}\, \mathrm{d}\Omega \tag{24}$$

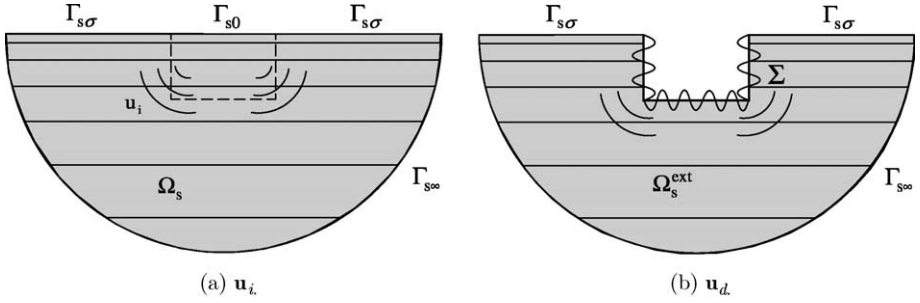

Fig. A.3. Decomposition of the soil displacement field $\mathbf{u}_s$ into (a) the incident wave field $\mathbf{u}_i$, and (b) the diffracted wave field $\mathbf{u}_d$.

Decompositions (5) and (11) are introduced into the variational formulation (24). A standard Galerkin procedure, using an analogous modal decomposition for the virtual displacement field $\mathbf{v} = \sum_{n=1}^{q} \boldsymbol{\psi}_n \delta\alpha_n$, with $\delta\alpha_n$ the virtual modal coordinates, results into the following system of equations for the modal coordinates $\boldsymbol{\alpha}$:

$$[\mathbf{K}_b - \omega^2 \mathbf{M}_b + \mathbf{K}_s]\boldsymbol{\alpha} = \mathbf{f}_b + \mathbf{f}_s \tag{25}$$

The stiffness and mass matrices $\mathbf{K}_b$ and $\mathbf{M}_b$ are equal to:

$$[\mathbf{K}_b]_{nm} = \int_{\Omega_b} \boldsymbol{\varepsilon}(\boldsymbol{\psi}_n) : \boldsymbol{\sigma}_b(\boldsymbol{\psi}_m)\, \mathrm{d}\Omega \tag{26}$$

$$[\mathbf{M}_b]_{nm} = \int_{\Omega_b} \boldsymbol{\psi}_n \cdot \rho_b \boldsymbol{\psi}_m\, \mathrm{d}\Omega \tag{27}$$

The impedance matrix of the soil $\mathbf{K}_s$ is equal to:

$$[\mathbf{K}_s]_{nm} = \int_{\Sigma} \boldsymbol{\psi}_n \cdot \mathbf{t}_s(\mathbf{u}_{dm})\, \mathrm{d}\Sigma \tag{28}$$

The vector $\mathbf{f}_b$ due to the external forces on the structure is defined as:

$$[\mathbf{f}_b]_n = \int_{\Gamma_{b\sigma}} \boldsymbol{\psi}_n \cdot \bar{\mathbf{t}}_b\, \mathrm{d}\Gamma + \int_{\Omega_b} \boldsymbol{\psi}_n \cdot \rho_b \mathbf{b}\, \mathrm{d}\Omega \tag{29}$$

The force vector $\mathbf{f}_s$ due to the incident wave field on the structure is equal to:

$$[\mathbf{f}_s]_n = -\int_{\Sigma} \boldsymbol{\psi}_n \cdot \mathbf{t}_s(\mathbf{u}_i + \mathbf{u}_{d0})\, \mathrm{d}\Sigma \tag{30}$$

The tractions $\mathbf{t}_s(\mathbf{u}_{dm})$ due to an imposed displacement field $\boldsymbol{\psi}_m$ on the interface Σ in the expression (28) for the soil impedance matrix are calculated using a boundary element formulation for the unbounded soil domain Ω_s^{ext}, resulting in fictitious eigenfrequencies that correspond to the eigenfrequencies of the interior soil domain Ω_s^{int}. Similarly, the calculation of the tractions $\mathbf{t}_s(\mathbf{u}_{d0})$ in expression (30) with a boundary element formulation gives rise to the same fictitious eigenfrequencies.

In Section 3, the boundary integral equation is derived and a procedure to mitigate the problem of fictitious eigenfrequencies is proposed.

3. The boundary integral equation for the displacement vector

The derivation of the boundary integral equation for exterior problems is based on the elastodynamic representation theorem defined on the entire soil domain $\Omega_s = \Omega_s^{\text{ext}} \cup \Omega_s^{\text{int}}$ before excavation (Fig A.2c). In order to explain how fictitious frequencies arise at the resonance frequencies of the interior soil domain Ω_s^{int}, the relationship between the classical direct boundary integral equation and the indirect formulation is first recalled.

3.1. The boundary integral equation for the displacement

The displacement $u_i(\boldsymbol{\xi})$ in a point $\boldsymbol{\xi}$ that is not located on the boundary Σ is written as a function of the displacement and traction jumps $[u_j](\mathbf{x})$ and $[t_j(\mathbf{u})](\mathbf{x})$ across the boundary Σ and the Green's displacement and traction tensors $u_{ij}^G(\boldsymbol{\xi}, \mathbf{x})$ and $t_{ij}^G(\boldsymbol{\xi}, \mathbf{x})$:

$$u_i(\boldsymbol{\xi}) = \int_{\Sigma} [t_j(\mathbf{u})](\mathbf{x}) u_{ij}^G(\boldsymbol{\xi}, \mathbf{x})\, \mathrm{d}\Sigma - \int_{\Sigma} t_{ij}^G(\boldsymbol{\xi}, \mathbf{x})[u_j](\mathbf{x})\, \mathrm{d}\Sigma \quad \text{with } \boldsymbol{\xi} \notin \Sigma \tag{31}$$

The displacement jump $[u_j](\mathbf{x})$ is defined as:

$$[u_j](\mathbf{x}) = u_j^{\text{ext}}(\mathbf{x}) - u_j^{\text{int}}(\mathbf{x}) \tag{32}$$

while the traction jump $[t_j(\mathbf{u})](\mathbf{x})$ is equal to:

$$[t_j(\mathbf{u})](\mathbf{x}) = t_j^{\text{int}}(\mathbf{u})(\mathbf{x}) + t_j^{\text{ext}}(\mathbf{u})(\mathbf{x}) = \sigma_{ij}^{\text{int}}(\mathbf{u})(\mathbf{x}) n_i^{\text{int}} + \sigma_{ij}^{\text{ext}}(\mathbf{u})(\mathbf{x}) n_i^{\text{ext}} \tag{33}$$

with n_i^{ext} and n_i^{int} the unit outward normal vectors to the exterior and interior domains Ω_s^{ext} and Ω_s^{int}, respectively (Fig. A.2b and A.2c). As the tractions $\mathbf{t}_s(\mathbf{u}_{dm})$ in the soil impedance matrix and the tractions $\mathbf{t}_s(\mathbf{u}_{d0})$ in the force vector are defined on the exterior soil domain Ω_s^{ext}, the unit outward normal vector $n_i^{\text{ext}} = n_i$ is preferred, and the traction jump becomes:

$$[t_j(\mathbf{u})](\mathbf{x}) = \sigma_{ij}^{\text{ext}}(\mathbf{u})(\mathbf{x}) n_i - \sigma_{ij}^{\text{int}}(\mathbf{u})(\mathbf{x}) n_i \tag{34}$$

The second-order Green's tensor $u_{ij}^G(\boldsymbol{\xi}, \mathbf{x})$ represents the displacement components in the direction $\mathbf{e}_j$ in the point $\mathbf{x}$ due to a Dirac load in the direction $\mathbf{e}_i$ at the point $\boldsymbol{\xi}$. The second-order Green's tensor $t_{ij}^G(\boldsymbol{\xi}, \mathbf{x})$ represents the components of the traction vector in the direction $\mathbf{e}_j$ in the point $\mathbf{x}$ for the same load. On a boundary with a unit outward normal vector n_k, these tractions are equal to $\sigma_{jk}^{Gi}(\boldsymbol{\xi}, \mathbf{x}) n_k$, with σ_{jk}^{Gi} the stress tensor.

The Green's displacements $u_{ij}^G(\boldsymbol{\xi}, \mathbf{x})$ show a weak singularity of order r^{-1} in the neighborhood of the point $\boldsymbol{\xi} = \mathbf{x}$ on the interface Σ, while the Green's tractions $t_{ij}^G(\boldsymbol{\xi}, \mathbf{x})$ show a strong singularity of order r^{-2}. Particular attention is therefore paid to the second integral on the right hand side of Eq. (31) when $\boldsymbol{\xi}$ approaches the interface Σ from the inside. This integral is therefore decomposed into two integrals on $\Sigma \backslash \Sigma_\varepsilon$ and Σ'_ε. The boundary Σ_ε is defined as $\Sigma \cap B_\varepsilon$ with B_ε a spherical extension of the interior domain Ω_s^{int} with center $\boldsymbol{\xi}$ and radius ε (Fig. A.4). The boundary $\Sigma'_\varepsilon = \partial B_\varepsilon \backslash (\partial B_\varepsilon \cap \Omega_s^{\text{int}})$ is the extension of the boundary of the interior domain Ω_s^{int}.

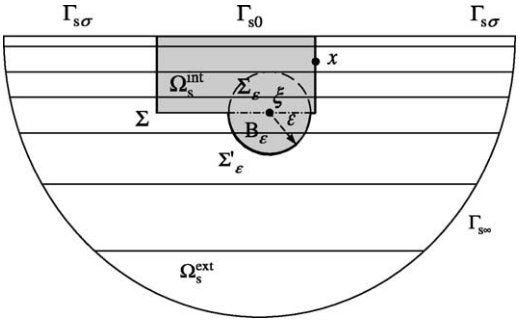

Fig. A.4. Expansion of the interior soil domain Ω_s^{int} with a sphere B_ε.

For $\xi \in \Sigma$ and for a smooth jump $[u_j]$, Eq. (31) results in:

$$u_i^{int}(\xi) = \int_\Sigma [t_j(\mathbf{u})](\mathbf{x}) u_{ij}^G(\xi,\mathbf{x})\, d\Sigma - c_{ij}(\xi)[u_j](\xi) - \oint_\Sigma t_{ij}^G(\xi,\mathbf{x})[u_j](\mathbf{x})\, d\Sigma \quad (35)$$

The integral free term $c_{ij}(\xi)$ is defined as the following limit:

$$c_{ij}(\xi) = \lim_{\varepsilon\to 0+} \int_{\Sigma'_\varepsilon} t_{ij}^G(\xi,\mathbf{x})\, d\Sigma \quad (36)$$

For a locally smooth boundary and a locally homogeneous domain at the point ξ, $c_{ij}(\xi) = \delta_{ij}/2$ [2,28].

The second integral on the right hand side of Eq. (35) is a Cauchy Principal Value (CPV) integral defined as:

$$\oint_\Sigma t_{ij}^G(\xi,\mathbf{x})[u_j](\mathbf{x})\, d\Sigma = \lim_{\varepsilon\to 0+} \int_{\Sigma\setminus\Sigma_\varepsilon} t_{ij}^G(\xi,\mathbf{x})[u_j](\mathbf{x})\, d\Sigma \quad (37)$$

3.2. Regularization of the boundary integral equation for the displacement

Rizzo and Shippy [29] and Bui and Bonnet [30,31] introduce a regularization procedure for a homogeneous halfspace; a similar procedure is proposed by Clouteau [2] and Aubry and Clouteau [28] for a layered halfspace. In both formulations, the evaluation of the CPV integral and the integral free term $c_{ij}(\xi)$ in Eq. (37) is avoided.

A zero traction static rigid body condition is applied to the boundary integral equation (35) [2,28]. The integral free term $c_{ij}(\xi)$ is given by:

$$c_{ij}(\xi) = \delta_{ij} - \oint_{\Sigma\cup\Gamma_{s0}} t_{ij}^{GS}(\xi,\mathbf{x})\, d\Sigma \quad (38)$$

where $t_{ij}^{GS}(\xi,\mathbf{x})$ represents the static Green's traction tensor. Eq. (38) is subsequently introduced into Eq. (37) and the following weakly singular boundary integral equation is obtained:

$$u_i^{int}(\xi) = \int_\Sigma [t_j(\mathbf{u})](\mathbf{x}) u_{ij}^G(\xi,\mathbf{x})\, d\Sigma - [u_i](\xi) - \int_\Sigma t_{ij}^{GS}(\xi,\mathbf{x})\{[u_j](\mathbf{x}) - [u_j](\xi)\}\, d\Sigma - \int_\Sigma \{t_{ij}^G(\xi,\mathbf{x}) - t_{ij}^{GS}(\xi,\mathbf{x})\}[u_j](\mathbf{x})\, d\Sigma \quad (39)$$

Whereas an analytical expression for the static Green's tensor $t_{ij}^{GS}(\xi,\mathbf{x})$ of a homogeneous halfspace is available, this is not the case for a layered halfspace and a numerical evaluation becomes necessary. Therefore, Clouteau [2] and Aubry and Clouteau [28,32] propose to use regularizing tensors. If the heterogeneous halfspace is locally homogeneous in the vicinity of the source point ξ, the static Green's tensor of a homogeneous full space, based on the material characteristics in the vicinity of the source point ξ, is used. However, the integral over Γ_{s0} has to be accounted for in Eq. (39).

Guzina and Pak [7] use a similar approach to treat the singularities in the displacement boundary integral equation for a layered halfspace. The integral equation is decomposed into a singular part for the near field, and a residual component for the mid to far field. Analytical expressions for the singular components of the dynamic Green's tensors are known as they are equal to the static solution for a bi-material full space, composed of two bonded elastic halfspaces with different material characteristics [33]. Therefore, the singular parts can be evaluated analytically. The remaining residual parts, corresponding to the mid to far field components, are evaluated numerically using contour integration. A modified path of integration is used to account for the poles.

3.3. The boundary integral equation for exterior problems

The boundary integral equation for exterior problems is obtained from Eq. (35) stating that u_j^{int} vanishes on Σ. Indeed, if it is assumed that $u_j^{int} = 0$ on Σ and $t_j^{int}(\mathbf{u}) = 0$ on Γ_{s0}, this implies a zero displacement field inside the interior domain Ω_s^{int}. The traction field in the interior domain Ω_s^{int} also vanishes and the two jumps $[u_j](\mathbf{x})$ and $[t_j(\mathbf{u})](\mathbf{x})$ are equal to the displacement and traction fields $u_j^{ext}(\mathbf{x})$ and $t_j^{ext}(\mathbf{u})(\mathbf{x})$ on the boundary Σ. Accounting for this in Eq. (35) gives:

$$\int_\Sigma t_j^{ext}(\mathbf{u})(\mathbf{x}) u_{ij}^G(\xi,\mathbf{x})\, d\Sigma = c_{ij}(\xi) u_j^{ext}(\xi) + \oint_\Sigma t_{ij}^G(\xi,\mathbf{x}) u_j^{ext}(\mathbf{x})\, d\Sigma \quad (40)$$

The regularized version of this equation is equal to:

$$u_i^{\text{ext}}(\xi) = \int_\Sigma t_j^{\text{ext}}(\mathbf{u})(\mathbf{x}) u_{ij}^G(\xi,\mathbf{x})\,\mathrm{d}\Sigma - \int_\Sigma t_{ij}^{GS}(\xi,\mathbf{x})\{u_j^{\text{ext}}(\mathbf{x}) - u_j^{\text{ext}}(\xi)\}\,\mathrm{d}\Sigma - \int_\Sigma \{t_{ij}^G(\xi,\mathbf{x}) - t_{ij}^{GS}(\xi,\mathbf{x})\} u_j^{\text{ext}}(\mathbf{x})\,\mathrm{d}\Sigma \tag{41}$$

The derivation of the boundary integral equations (40) or (41) for problems defined on the exterior soil domain Ω_s^{ext} is based on the assumption that the displacements u_j^{int} are equal to zero for all points ξ on the boundary Σ and thus in the interior domain Ω_s^{int}. The displacements u_i^{int} vanish everywhere in Ω_s^{int} as long as the elastodynamic boundary value problem for an interior domain Ω_s^{int} with zero displacement boundary conditions on Σ and zero traction boundary conditions on Γ_{s0} has a unique solution. Unfortunately, the solution is not unique when the excitation frequency ω is equal to one of the eigenfrequencies $\bar{\omega}_k$ of the interior domain (with zero displacement boundary conditions on Σ and zero traction boundary conditions on Γ_{s0}) and, consequently, $t_j^{\text{int}}(\mathbf{u})(\xi)$ does not necessary vanish at these frequencies, leading to an ill-posed boundary integral equation.

4. The boundary integral equation for the displacement gradient

Burton and Miller's [14] original formulation for acoustic problems is based on a linear combination of the integral equations for the pressure and the normal velocity. In elastodynamics, the traction vector on a boundary is obtained from the projection of the stress tensor on the unit normal vector on the boundary. The stress tensor is related by the constitutive equations to the strain tensor, that is defined in terms of the displacement gradient or, alternatively, as a function of the normal and tangential derivatives of the displacement vector along a boundary.

For reasons of simplicity, it is preferred herein not to explicitly evaluate the traction vector along the boundary in terms of the normal and tangential derivatives but to use only the normal derivatives of the displacement vector along the boundary since this term is providing additional information to the known displacement field on Σ.

In this section, the boundary integral equation for the normal derivative of the displacements $u_i(\xi)$ is evaluated. Differentiating the displacement boundary integral equation (40) with respect to the spatial coordinates ξ_k is particularly unsafe, however, since this equation is only defined for points on the boundary Σ. Therefore, the differentiation is performed on the displacement boundary integral equation (31) and the limit for ξ approaching the boundary Σ is evaluated. The normal derivative is defined as follows from Eq. (35) in the case of a smooth surface and regular jumps $[u_j]$ and $[t_j(\mathbf{u})]$ on Σ and for a homogeneous space:

$$u_{i,k}^{\text{int}}(\xi) n_k = \int_\Sigma [t_j(\mathbf{u})](\mathbf{x}) u_{ij,k}^G(\xi,\mathbf{x}) n_k\,\mathrm{d}\Sigma - c_{ij}(\xi)[u_{j,k} n_k](\xi) - \text{⨍}_\Sigma t_{ij,k}^G(\xi,\mathbf{x}) n_k [u_j](\mathbf{x})\,\mathrm{d}\Sigma \tag{42}$$

The kernels $u_{ij,k}^G(\xi,\mathbf{x})$ and $t_{ij,k}^G(\xi,\mathbf{x})$ have singularities of order r^{-2} and r^{-3} at the point $\xi = \mathbf{x}$ on the boundary Σ, respectively. As a consequence, the first integral on the right hand side of Eq. (42) only exist as a CPV integral, while the second integral is hypersingular and defined as a Hadamard Finite Part integral [34], denoted by ⨍. As the aim of this section is not to give a complete review on highly singular boundary integrals, the reader is referred to the work of Bonnet [8] for more detailed developments.

The boundary integral equation for the normal derivative of the displacement consists of stating that $u_{i,k}^{\text{int}}(\xi) n_k = 0$ on the boundary Σ. It is assumed that this condition and the traction-free condition on Γ_{s0} imply that, for an elastodynamic field, the displacements $u_i^{\text{int}}(\xi)$ in the interior domain Ω_s^{int} are equal to zero, resulting also in vanishing tractions $t_i^{\text{int}}(\mathbf{u})(\mathbf{x})$ in the interior domain. Therefore, the displacement jump $[u_j](\mathbf{x})$ is equal to the displacement $u_i^{\text{ext}}(\mathbf{x})$, while the traction jump $[t_i(\mathbf{u})](\mathbf{x})$ reduces to $t_i^{\text{ext}}(\mathbf{u})(\mathbf{x})$, leading to the boundary integral equation for the normal derivatives of the displacement:

$$\text{⨍}_\Sigma t_j^{\text{ext}}(\mathbf{u})(\mathbf{x}) u_{ij,k}^G(\xi,\mathbf{x}) n_k\,\mathrm{d}\Sigma = c_{ij}(\xi) u_{j,k}^{\text{ext}}(\xi) n_k + \text{⨍}_\Sigma t_{ij,k}^G(\xi,\mathbf{x}) u_j^{\text{ext}}(\mathbf{x}) n_k\,\mathrm{d}\Sigma \tag{43}$$

Regularized forms of this equation have been proposed for a homogeneous halfspace [8,35] but, to the authors' knowledge, similar expressions are not available for a layered halfspace. It is not even sure that the integral free term $c_{ij}(\xi)$ in Eq. (43) is the same as in Eq. (40).

The static Green's tensors for a bi-material composed of two bonded elastic halfspaces with different material characteristics have been used by Guzina and Pak [7,33] to isolate the singular part in the displacement boundary integral equation. These static Green's tensors might be a useful ingredient for a similar regularization of the boundary integral equation (43) for the displacement gradient. However, the singularities in the Green's tensors $u_{ij,k}^G(\xi,\mathbf{x})$ and $t_{ij,k}^G(\xi,\mathbf{x})$ are of higher order, which would necessitate further investigations.

The solution of the boundary integral equation (43) for the normal derivatives of the displacement is not unique for exterior problems. When the frequency ω is equal to one of the eigenfrequencies $\bar{\omega}_k'$ of the interior domain with

the normal derivative of the displacement equal to zero on Σ and a zero traction boundary condition on Γ_{s0}, the solution is not unique.

5. The combined boundary integral equation

As the fictitious eigenfrequencies corresponding to the boundary integral equations (40) and (43) are different, a different boundary condition could be used at each fictitious frequency to mitigate the problem of fictitious frequencies. In order to obtain a well-posed boundary integral equation at all frequencies, however, a linear combination of the boundary integral equation (37) for the displacement $u_i^{\text{int}}(\boldsymbol{\xi})$ and of the boundary integral equation (42) for the displacement gradient $u_{i,k}^{\text{int}}(\boldsymbol{\xi})n_k$ along the normal direction of the boundary is classically preferred, corresponding to the following mixed boundary condition on the boundary Σ for the displacement field $u_i^{\text{int}}(\boldsymbol{\xi})$:

$$u_i^{\text{int}}(\boldsymbol{\xi}) + \alpha u_{i,k}^{\text{int}}(\boldsymbol{\xi})n_k = 0 \quad \text{on } \Sigma \tag{44}$$

where α is a complex coupling parameter with the dimension of a length. Upon the introduction of the boundary integral equations (37) and (42) into the mixed boundary equation (44), the following boundary integral equation is obtained:

$$\int_\Sigma [t_j(\mathbf{u})](\mathbf{x})u_{ij}^G(\boldsymbol{\xi},\mathbf{x})\,\mathrm{d}\Sigma + \alpha \int_\Sigma [t_j(\mathbf{u})](\mathbf{x})u_{i,k}^G(\boldsymbol{\xi},\mathbf{x})n_k\,\mathrm{d}\Sigma$$
$$- c_{ij}(\boldsymbol{\xi})([u_j](\boldsymbol{\xi}) + \alpha[u_j]_{,k}n_k(\boldsymbol{\xi})) - \int_\Sigma t_{ij}^G(\boldsymbol{\xi},\mathbf{x})[u_j](\mathbf{x})\,\mathrm{d}\Sigma$$
$$- \alpha \oint_\Sigma t_{ij,k}^G(\boldsymbol{\xi},\mathbf{x})n_k[u_j](\mathbf{x})\,\mathrm{d}\Sigma = 0 \tag{45}$$

A very small value of α results in the original boundary integral equation (37), whereas the boundary integral equation (42) for the displacement gradient along the normal direction on the boundary is recovered for very large values of α. The real part of α corresponds to a compliance boundary condition on the boundary Σ if the traction boundary integral equation were used. Its imaginary part is equivalent to the inverse of a wave number, resulting in an absorbing boundary condition on the boundary Σ. As it is shown in Appendix A, fictitious eigenfrequencies can be avoided using the mixed boundary condition (44), provided that the coupling parameter α has a non-zero positive imaginary part: real eigenfrequencies for the interior boundary value problem no longer exist, resulting in a unique solution.

Since a zero displacement field is such a solution inside the interior domain Ω_s^{int}, the traction field in the interior domain Ω_s^{int} also vanishes and the two jumps $[u_j](\mathbf{x})$ and $[t_j(\mathbf{u})](\mathbf{x})$ in Eq. (45) are equal to the displacement and traction fields $u_j^{\text{ext}}(\mathbf{x})$ and $t_j^{\text{ext}}(\mathbf{u})(\mathbf{x})$ on the boundary Σ. The boundary integral equation for exterior problems becomes:

$$\int_\Sigma t_j^{\text{ext}}(\mathbf{u})(\mathbf{x})u_{ij}^G(\boldsymbol{\xi},\mathbf{x})\,\mathrm{d}\Sigma + \alpha \int_\Sigma t_j^{\text{ext}}(\mathbf{u})(\mathbf{x})u_{ij,k}^G(\boldsymbol{\xi},\mathbf{x})n_k\,\mathrm{d}\Sigma$$
$$- c_{ij}(\boldsymbol{\xi})(u_j^{\text{ext}}(\boldsymbol{\xi}) + \alpha u_{j,k}^{\text{ext}}n_k(\boldsymbol{\xi})) - \int_\Sigma t_{ij}^G(\boldsymbol{\xi},\mathbf{x})u_j^{\text{ext}}(\mathbf{x})\,\mathrm{d}\Sigma$$
$$- \alpha \oint_\Sigma t_{ij,k}^G(\boldsymbol{\xi},\mathbf{x})n_k u_j^{\text{ext}}(\mathbf{x})\,\mathrm{d}\Sigma = 0 \tag{46}$$

Amini [15] has analyzed the choice of the coupling parameter α in Burton and Miller's boundary integral formulation for acoustic problems [14]. The condition number of the linear operators is a function of the eigenvalues of the boundary integral operators and has to be minimized. For interior domains with a simple geometry (e.g. a sphere), the smallest condition number is obtained for a coupling parameter α that is inversely proportional to the wave number $k_p = \omega/C_p$ of the longitudinal waves. In elastodynamic problems, the wave number $k_s = \omega/C_s$ of the shear waves can be chosen alternatively. In this paper, an imaginary coupling parameter $\alpha = i/k_s$ is used. Similar results are expected when the longitudinal wave number k_p is used for the calculation of the normal stress component and the shear wave number k_s for the transverse components.

A dimensionless coupling parameter $\bar{\alpha}$ is subsequently introduced, defined as the ratio of the parameter α and a characteristic length R of the interior domain (e.g. the radius of an embedded foundation):

$$\bar{\alpha} = \frac{\alpha}{R} = \frac{i}{k_s R} = \frac{iC_s}{\omega R} = \frac{i}{a_0} \tag{47}$$

where $a_0 = \omega R/C_s$ is a dimensionless frequency.

6. Finite difference approximation of the mixed boundary integral equation

The boundary integral equation (46) is hypersingular and would require advanced regularization techniques that are believed to be still unavailable for a layered halfspace. In order to avoid the evaluation of these hypersingular terms, while preserving the well-posedness of the problem at all frequencies, it is proposed to use a finite difference approximation on the derivatives of the displacement and traction fields along the direction normal to the boundary:

$$u_j^{\text{int}}(\boldsymbol{\xi}) + \alpha \frac{u_j^{\text{int}}(\boldsymbol{\xi}) - u_j^{\text{int}}(\boldsymbol{\xi} - h\boldsymbol{n}(\boldsymbol{\xi}))}{h} = 0 \tag{48}$$

where h is the distance between the boundary Σ and a second boundary Σ^-, located in the interior soil domain Ω_s^{int} and defined as $\Sigma^- = \{\boldsymbol{\xi}^- = \boldsymbol{\xi} - h\boldsymbol{n}(\boldsymbol{\xi});\ \boldsymbol{\xi} \in \Sigma\} \subset \Omega_s^{\text{int}}$.

Applying this finite difference approximation (48) to equation (46) finally results in the following boundary integral equation that only contains the Green's functions $u_{ij}^G(\boldsymbol{\xi},\mathbf{x})$ and $t_{ij}^G(\boldsymbol{\xi},\mathbf{x})$:

$$c_{ij}(\boldsymbol{\xi})u_j^{\text{ext}}(\boldsymbol{\xi}) = \int_\Sigma t_j^{\text{ext}}(\mathbf{u})(\mathbf{x})\left(u_{ij}^G(\boldsymbol{\xi},\mathbf{x}) - \frac{\alpha}{h+\alpha}u_{ij}^G(\boldsymbol{\xi}^-,\mathbf{x})\right)\mathrm{d}\Sigma - \int_\Sigma \left(t_{ij}^G(\boldsymbol{\xi},\mathbf{x}) - \frac{\alpha}{h+\alpha}t_{ij}^G(\boldsymbol{\xi}^-,\mathbf{x})\right)u_j^{\text{ext}}(\mathbf{x})\,\mathrm{d}\Sigma \tag{49}$$

This combined boundary integral equation eliminates fictitious eigenfrequencies and can easily be implemented in a boundary element formulation, as will be demonstrated in Section 7. It can also be regularized using the same technique as for Eq. (35).

Based on the previous developments, demonstrating that Eq. (49) has no fictitious eigenfrequencies is equivalent to proving that the elastodynamic problem in the interior domain Ω_s^{int} with the non-local boundary condition (48) has a unique solution. The proof of the uniqueness is given in Appendix A where it is shown that if α has a non-zero imaginary part and if h is small enough, a purely real eigenfrequency for the interior problem with the mixed boundary condition (48) can only be obtained when $u_i^{\text{int}}(\boldsymbol{\xi}) = u_i^{\text{int}}(\boldsymbol{\xi} - h\boldsymbol{n}(\boldsymbol{\xi})) = 0$, i.e. for eigenmodes of the Dirichlet problem defined on the elastic layer trapped between the boundaries Σ and Σ^-. The maximum excitation frequency $\omega_{\max}$ has to be smaller than a frequency $\omega_c(h)$, that is related to the distance h between the boundaries Σ and Σ^-. If the boundary Σ is smooth and if the distance h is small, the smallest eigenfrequency $\omega_c(h)$ of this elastic layer has an order of magnitude equal to $2\pi C_s/2h$, where C_s is the shear wave velocity. In Section 7, this distance h will be related to the size l_e of an individual boundary element.

7. Boundary element implementation

The interface Σ between the foundation and the soil is discretized into boundary elements. The tractions and displacements on the interface Σ are interpolated using nodal values and element based shape functions and the boundary integral is evaluated numerically for each element.

The classical boundary element formulation results in the following system of equations:

$$\mathbf{H}\underline{\mathbf{u}} = \mathbf{G}\underline{\mathbf{t}} \tag{50}$$

where the coefficient matrices $\mathbf{G}$ and $\mathbf{H}$ are fully populated and non-symmetric matrices and represent the Green's displacement and traction tensor, respectively. $\underline{\mathbf{t}}$ and $\underline{\mathbf{u}}$ are the nodal traction and displacement vectors.

The boundary element discretization applied to the boundary integral equation (49) simply consists in adding a regular term for sources $\boldsymbol{\xi}^-$ the boundary Σ^-. The resulting system of equations reads as:

$$\left(\mathbf{H} + \frac{\alpha}{h+\alpha}\mathbf{H}^-\right)\underline{\mathbf{u}} = \left(\mathbf{G} + \frac{\alpha}{h+\alpha}\mathbf{G}^-\right)\underline{\mathbf{t}} \tag{51}$$

The computation of the matrices $\mathbf{G}^-$ and $\mathbf{H}^-$, corresponding to the sources $\boldsymbol{\xi}^-$ on the boundary Σ^-, increases the computational effort. This approach is quite generic for any type of Green's function and for collocation as well as variational approaches. It is easy to implement in an existing boundary element program as it only requires a second computation for the inner sources on the boundary Σ^- and does not modify the structure and the size of the original system of equations.

Terms in Eq. (49) are subject to strong numerical errors if the distance h between the boundaries Σ^- and Σ is small: if the position $\boldsymbol{\xi}^-$ of the source on the boundary Σ^- approaches the position $\mathbf{x}$ of the receiver on the boundary Σ, the Green's tensors $u_{ij}^G(\boldsymbol{\xi}^-,\mathbf{x})$ and $t_{ij}^G(\mathbf{u})(\boldsymbol{\xi}^-,\mathbf{x})$ show singularities of the order r^{-1} and r^{-2}, respectively. The integrals become nearly singular and would require an appropriate integration scheme. Therefore, the distance h is chosen larger than the size l_e of a boundary element, estimated as the square root of the maximum surface of a boundary element on the interface Σ between the soil and the structure. It is convenient to introduce the dimensionless distance $\bar{h}$ as the ratio of the distance h and the size l_e of a boundary element:

$$\bar{h} = \frac{h}{l_e} \tag{52}$$

The distance h also has to be small enough as to ensure that the boundary Σ^- is located inside the interior domain Ω_s^{int}, which gives another argument to relate the distance h to the size l_e of a boundary element. For relatively thin embedded structures, the choice of values $\bar{h}$ larger than 1 involves the risk of defining points $\boldsymbol{\xi}^-$ outside the interior domain Ω_s^{int}.

Furthermore, the distance h should be strictly smaller than the smallest radius of curvature $r_{\min}$ of the boundary Σ. This condition prevents the use of the present formulation for non-smooth boundaries. However, one can always define a smooth field with pseudo-normal vectors instead of using the actual one in order to have an invertible mapping from Σ to Σ^-, this smoothing procedure being driven also by the mesh size.

In Section 6, it has been argued that the maximum excitation frequency $\omega_{\max}$ should remain smaller than the eigenfrequency $\omega_c(h)$ of the elastic layer trapped between the boundaries Σ and Σ^-. If the dimensionless distance $\bar{h} = 1$, this criterion imposes that the element size l_e should

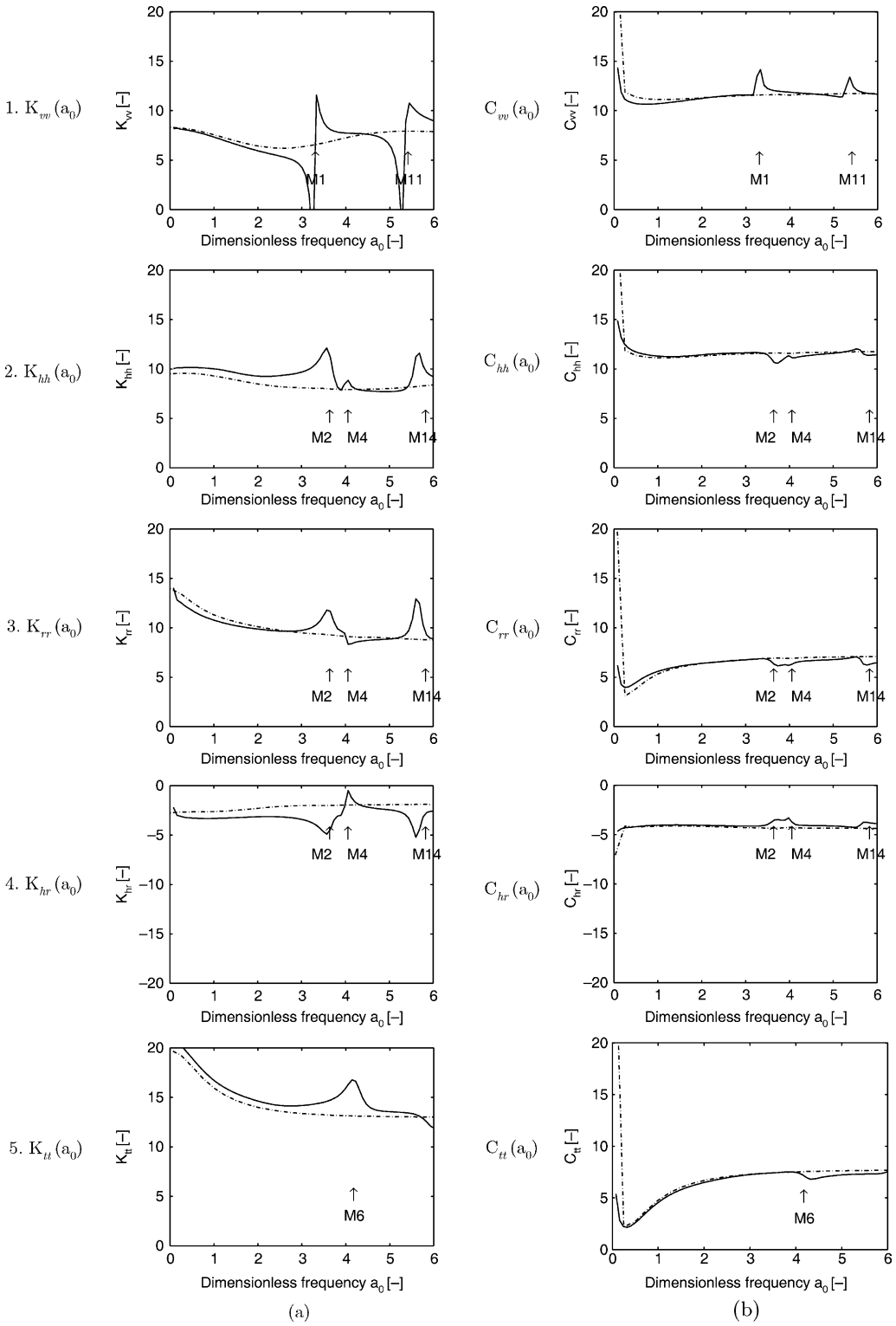

Fig. A.5. (a) Real part $K_{mn}(a_0)$ and (b) imaginary part $C_{mn}(a_0)$ of the dimensionless impedance functions as a function of the dimensionless frequency a_0 for $\bar{\alpha}=0$ (solid line) and according to Apsel and Luco [37] (dashed-dotted line).

remain smaller than $\lambda_{\min}/2$, with $\lambda_{\min}$ the minimum wavelength.

Besides, the boundary element size is also limited to $\lambda_{\min}/N_e$, with $\lambda_{\min}$ the minimum wavelength in the soil and N_e the number of elements per wavelength. A minimum value $N_e=6$ is strongly advisable [36]. This criterion is more strict than the previous criterion on the maximum excitation frequency, so that the latter is automatically fulfilled if an appropriate boundary element discretization is chosen.

8. Impedance of a rigid massless cylindrical embedded foundation

8.1. Problem outline

The solution technique proposed in the previous sections is now illustrated by means of a numerical example, where the impedance functions of a rigid massless cylindrical foundation embedded in a homogeneous soil are considered. Results are compared to results published by Apsel and Luco [37]. A parametric study allows to define guidelines for an appropriate choice of the dimensionless coupling parameter $\bar{\alpha}$ and the dimensionless distance $\bar{h}$.

A rigid massless cylindrical embedded foundation with a radius $R=1.94$ m and an embedment ratio $d/R=1.0$ is considered. The soil is modeled as a homogeneous halfspace and has a shear wave velocity $C_s=150$ m/s, a Poisson's ratio $\nu^s=0.25$, a density $\rho_s=1800$ kg/m^3 and a hysteretic material damping ratio $\beta_s=0.01$ in shear and longitudinal deformation.

The frequency dependent elements $S_{mn}(a_0)$ of the 6 by 6 impedance matrix of a rigid foundation are written in the following dimensionless form [38]:

$$S_{mn}(a_0) = K^s_{mn}[K_{mn}(a_0) + ia_0C_{mn}(a_0)] \tag{53}$$

where the subscripts m and n denote the horizontal (h), vertical (v), rotational (r) and torsional (t) degree of freedom, while the static stiffness coefficients K^s_{mn} are defined as $K^s_{hh}=K^s_{vv}=\mu R$, $K^s_{rr}=K^s_{tt}=\mu R^3$ and $K^s_{hr}=\mu R^2$, with $\mu=C_s^2\rho_s$ the shear modulus of the soil. The dimensionless functions $K_{mn}(a_0)$ and $C_{mn}(a_0)$ depend on the dimensionless frequency $a_0=\omega R/C_s$.

8.2. The reference solution

Apsel and Luco [37] use an integral equation based on the Green's functions of a layered viscoelastic halfspace to determine the impedance functions of three-dimensional rigid foundations subjected to external forces and moments. The boundary integral equation is defined on a boundary located in the interior domain. A distribution of sources on this boundary represents the unknowns. A non-singular integral equation with a symmetric kernel is obtained in terms of the unknown distribution of sources. For rigid foundations, the force distribution is written in terms of the unit rigid body displacements of the soil–foundation interface for each of the six degrees of freedom of the foundation, using a body force distribution matrix. The solution of the integral equation in terms of the body force distribution is accomplished by discretization, which reduces the integral equation to a set of linear algebraic equations.

The accuracy of the numerical solution of the integral equation is influenced by the number of source and receiver points and depends on the distance between the soil–foundation interface and the boundary in the interior soil domain. For an embedment ratio $d/R=1.0$, Apsel and Luco use 65 observation points and 29 source points. Only absolute values of the number of observation points as a function of the embedment ratio are given. The distance between the soil–foundation interface and the boundary in the interior domain is equal to $2.5d_{\text{obs}}$, with d_{obs} the distance between the observation points.

The dashed-dotted lines in Fig. A.5 show the real and imaginary parts $K_{mn}(a_0)$ and $C_{mn}(a_0)$ of the non-zero elements of the foundation's impedance matrix as computed by Apsel and Luco [37] for dimensionless frequencies up to $a_0^{\max}=6.0$, corresponding to an excitation frequency of 73.83 Hz. These solutions seem to be free of fictitious eigenfrequencies maybe because they are obtained with a boundary integral equation for exterior problems that is defined on a boundary located in the interior domain. Therefore, the solutions of Apsel and Luco will be used as a reference in the following.

As the dimensionless frequency a_0 is factored out in the imaginary part of the impedance functions $S_{mn}(a_0)$ in Eq. (53), due to hysteretical damping, the imaginary parts $C_{mn}(a_0)$ tend to very high values when the dimensionless frequency a_0 tends to zero.

8.3. Boundary element discretization

The impedance functions of the rigid embedded cylindrical foundation are calculated with a boundary element formulation. Fig. A.6 shows the discretization of the interface Σ between the foundation and the soil into 448 boundary elements. The size l_e of a boundary element is equal to 0.33 m so that $N_e=\lambda_{\min}/l_e=6$ boundary elements are used at the minimum wavelength $\lambda_{\min}$ of the shear wave in the soil; the latter is equal to 2 m for a shear wave velocity $C_s=150$ m/s and a maximum frequency $f_{\max}=75$ Hz.

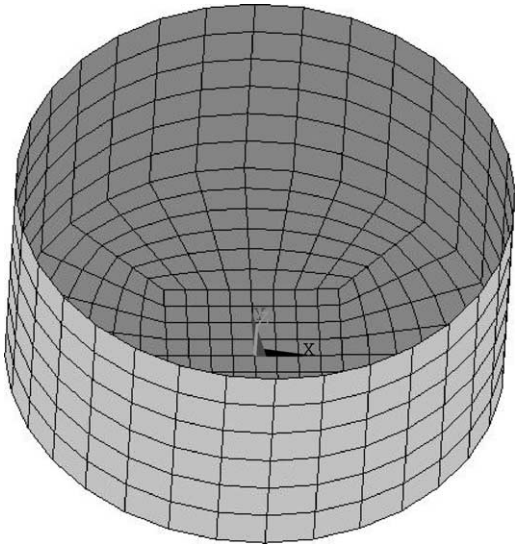

Fig. A.6. Boundary element discretization of the interface Σ between the foundation and the soil.

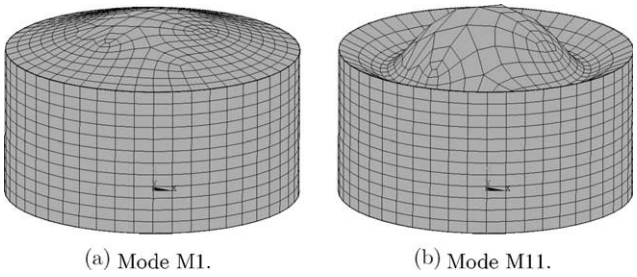

Fig. A.7. Vertical modes (a) M1 ($a_0=3.3$) and (b) M11 ($a_0=5.4$) of the interior soil domain Ω_s^{int}.

The traction field $\mathbf{t}(\mathbf{u})$ is approximated by a constant value over each boundary element and a collocation method is applied.

The Green's functions for the layered halfspace in the integral equations are calculated using Kennet's method [39], which is based on reflection and transmission coefficients. The Green's functions are computed in the wave number and frequency domain. The inverse Hankel transformations between the wave number and the spatial domain are performed with a constant quadrature step $\Delta\bar{k}_r = 0.007$ up to a value $\bar{k}_r^{\max} = 15$, where the dimensionless radial wave number is defined as $\bar{k}_r = k_r C_s/\omega$.

The regular integrals are evaluated with a Gauss quadrature rule with six Gauss points in each coordinate direction, while a special quadrature scheme with 256 points is used to evaluate the weakly singular integrals.

8.4. Appearance of fictitious eigenfrequencies

In order to demonstrate the problem associated with the appearance of fictitious eigenfrequencies, the elements $S_{mn}(a_0)$ of the impedance matrix of the rigid massless cylindrical embedded foundation are first computed using a boundary element formulation that is based on the displacement boundary integral equation (31). The dimensionless coupling parameter $\bar{\alpha}$ is equal to zero in this case.

Calculations are performed for dimensionless frequencies up to $a_0^{\max} = 6.0$ and a step $\Delta a_0 = 0.081$. Fig. A.5a and A.5b compares these results with the impedance functions obtained by Apsel and Luco, which are drawn in a dashed-dotted line on all figures.

Fig. A.5.1a and A.5.1b reveal important discrepancies between the computed real part $K_{vv}(a_0)$ and the imaginary part $C_{vv}(a_0)$ of the vertical impedance and the reference solutions at the dimensionless frequencies $a_0=3.3$ and $a_0=5.4$. These anomalies are labeled as M1 and M11 and are associated with fictitious eigenfrequencies corresponding to the eigenfrequencies of the interior soil domain Ω_s^{int} with Dirichlet boundary conditions along the interface Σ and free boundary conditions along the free surface Γ_{s0}. In order to demonstrate this, the eigenfrequencies and eigenmodes of the interior soil domain Ω_s^{int} have been computed with a finite element model, consisting of linear eight node brick elements, with material properties corresponding to the excavated soil. Fig. A.7 shows the first two vertical eigenmodes M1 and M11 of the interior soil domain Ω_s^{int} at the dimensionless frequencies $a_0=3.3$ and $a_0=5.4$. The discrepancy between the computed damping coefficient $C_{mn}(a_0)$ and the reference solution is amplified at low values of the dimensionless frequency a_0 since the dimensionless frequency a_0 has been factored out in Eq. (53).

Fig. A.8 shows the displacements at the dimensionless frequency $a_0=3.3$ in the points located at the free surface due to a unit vertical harmonic point load applied at the center of the base of the cylindrical foundation. The displacements are not only shown on the free surface $\Gamma_{s\sigma}$ of the exterior domain Ω_s^{ext}, but also on the free surface Γ_{s0} of the interior domain Ω_s^{int}. Large non-zero displacements can clearly be observed in the latter points and are associated with the spurious mode M1 at the fictitious eigenfrequency $a_0=3.3$.

Fig. A.5.2, A.5.3 and A.5.4 reveal similar discrepancies between the computed impedance functions for the horizontal, rocking and coupled horizontal–rocking vibration modes and the reference solutions at the dimensionless frequencies $a_0=3.6$, $a_0=4.0$ and $a_0=5.8$.

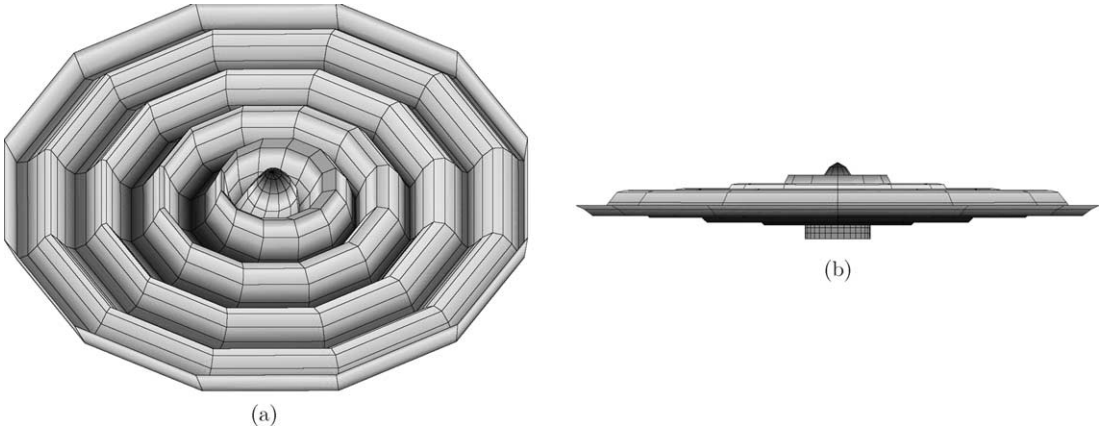

Fig. A.8. (a) Isometric and (b) side view of the displacements at points on the surface for the rigid massless cylindrical embedded foundation excited by a vertical harmonic point load at a dimensionless frequency $a_0=3.3$, computed with the parameter $\bar{\alpha}=0$.

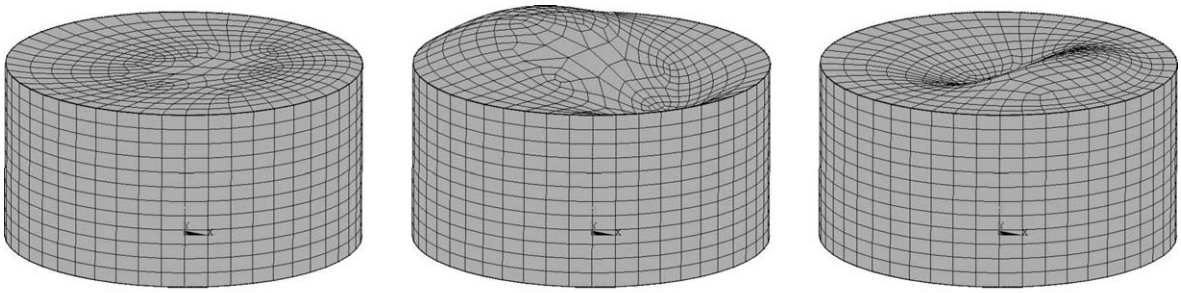

(a) Mode M2. (b) Mode M4. (c) Mode M14.

Fig. A.9. Horizontal and rocking modes (a) M2 ($a_0=3.6$), (b) M4 ($a_0=4.0$) and (c) M14 ($a_0=5.8$) of the interior soil domain Ω_s^{int}.

These anomalies are labeled as M2, M4 and M14 and are associated with fictitious eigenfrequencies corresponding to the horizontal and rocking modes of the interior soil domain Ω_s^{int} with Dirichlet boundary conditions along the interface Σ and free boundary conditions along the free surface Γ_{s0}, as illustrated in Fig. A.9. The first peak on the real part $K_{hh}(a_0)$ of the horizontal impedance at $a_0=3.6$ corresponds to the horizontal mode M2, while the peaks at $a_0=4.0$ and $a_0=5.8$, correspond to the rocking modes M4 and M14 of the interior soil domain. These three spurious modes influence the three impedance coefficients $K_{hh}(a_0)$, $K_{rr}(a_0)$ and $K_{hr}(a_0)$ (and, to a lesser extent, the corresponding imaginary parts $C_{hh}(a_0)$, $C_{rr}(a_0)$ and $C_{hr}(a_0)$) in the frequency range of interest due to the coupling between the horizontal and rocking motion.

Fig. A.5.5a and A.5.5b shows the real part $K_{tt}(a_0)$ and the imaginary part $C_{tt}(a_0)$ of the torsional impedance of the foundation. A single anomaly occurs at a dimensionless frequency $a_0=4.2$ that corresponds to the first torsional mode M6 of the interior soil domain Ω_s^{int} (Fig. A.10).

In the following subsections, it is demonstrated how this numerical problem can be mitigated by discretizing alternatively the combined boundary integral equation (49) along the interface Σ between the soil and the foundation. The choice of the dimensionless parameters $\bar{\alpha}$ and $\bar{h}$ is demonstrated to be crucial.

8.5. Choice of a frequency dependent dimensionless coupling parameter $\bar{\alpha}$

Following Amini's recommendations [15], a frequency dependent coupling parameter $\bar{\alpha}=i/a_0$ is first considered. The dimensionless parameter $\bar{h}=1$ is fixed in the following examples.

Fig. A.11a and A.11b compares the real and imaginary part of the dimensionless impedance functions for a frequency dependent coupling parameter $\bar{\alpha}=i/a_0$ and for a constant coupling parameter $\bar{\alpha}=i/6$ with the reference solutions of Apsel and Luco. An imaginary value of $\bar{\alpha}$ represents a damping condition on the boundary of the interior domain Ω_s^{int}. When $\bar{\alpha}$ is inversely proportional to the dimensionless frequency, a very large value of $\bar{\alpha}$ is obtained at small frequencies, resulting in an increasing contribution of the boundary integral equation for the displacement gradient and an increasing deviation of the computed impedance functions from the reference values. The discretization of the original displacement boundary integral would have resulted in sufficiently accurate results at low excitation frequencies, whereas now, a solution method is used in a frequency range where it is not needed and designed for: the first fictitious eigenfrequency is equal to $a_0=3.3$, corresponding to the first vertical mode of the interior soil domain. A frequency dependent coupling parameter is therefore avoided in the range of low dimensionless frequencies and a frequency independent dimensionless coupling parameter $\bar{\alpha}$ will be preferred in the following.

8.6. Choice of a frequency independent dimensionless coupling parameter $\bar{\alpha}$

Fig. A.12a and A.12b shows the real and imaginary part of the dimensionless impedance functions computed with $\bar{h}=1$ and the following values of a constant dimensionless coupling parameter: $\bar{\alpha}=i/6$, $\bar{\alpha}=i/3$ and $\bar{\alpha}=i/2$. The results obtained with $\bar{\alpha}=i/6$, corresponding to the maximum dimensionless frequency $a_0^{\max}=6$, are in good agreement with the results of Apsel and Luco, while the deviations increase for increasing values of $\bar{\alpha}$.

The next example illustrates what happens when the dimensionless coupling parameter $\bar{\alpha}$ is too large. Fig. A.13a and A.13b shows the real and imaginary part of

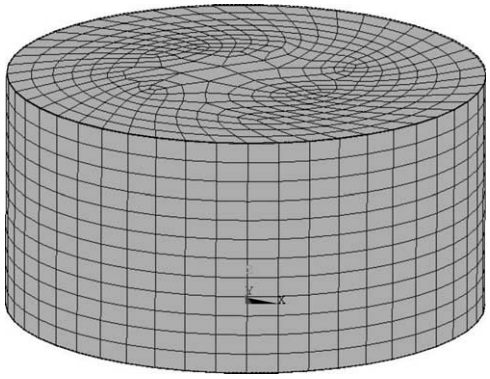

Fig. A.10. Torsional mode M6 ($a_0=4.2$) of the interior soil domain Ω_s^{int}.

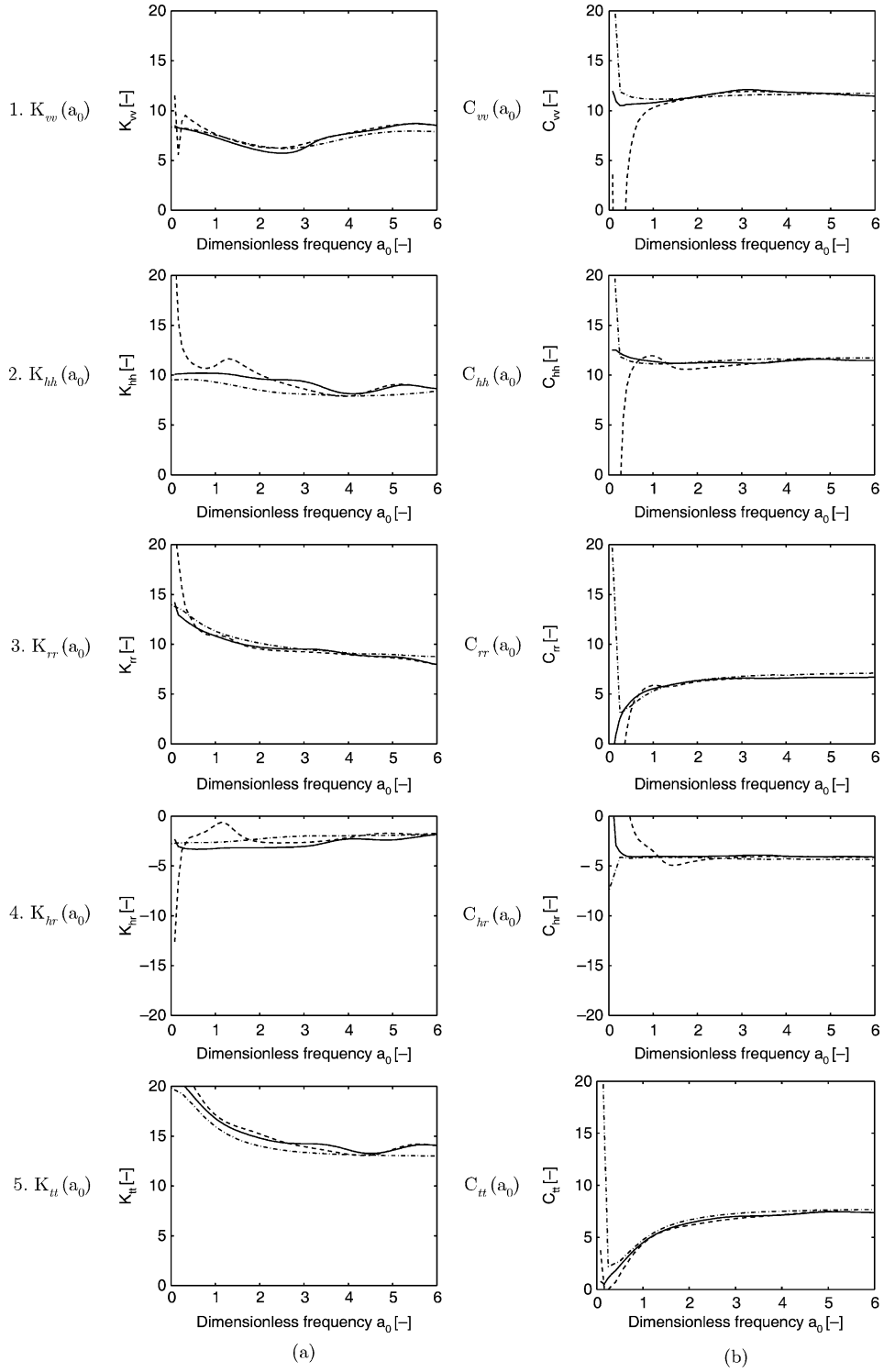

Fig. A.11. (a) Real part $K_{mn}(a_0)$ and (b) imaginary part $C_{mn}(a_0)$ of the dimensionless impedance functions as a function of the dimensionless frequency a_0 for $\bar{h} = 1$ and $\bar{\alpha} = i/6$ (solid line), for $\bar{h} = 1$ and $\bar{\alpha} = i/a_0$ (dashed line) and according to Apsel and Luco [37] (dashed-dotted line).

the dimensionless impedance functions computed with $\bar{h} = 1$ and a large dimensionless coupling parameter $\bar{\alpha} = 5i/3$. The contribution of the boundary integral equation for the displacement gradient along the normal direction dominates the combined boundary integral equation (49) and numerical problems occur at fictitious eigenfrequencies $\bar{\omega}'_k$ that correspond to the resonance frequencies of the interior soil domain Ω_s^{int} with boundary conditions $u_{i,k}^{\text{int}}(\xi)n_k = 0$ along the soil–structure interface Σ and free boundary conditions along the boundary Γ_{s0}.

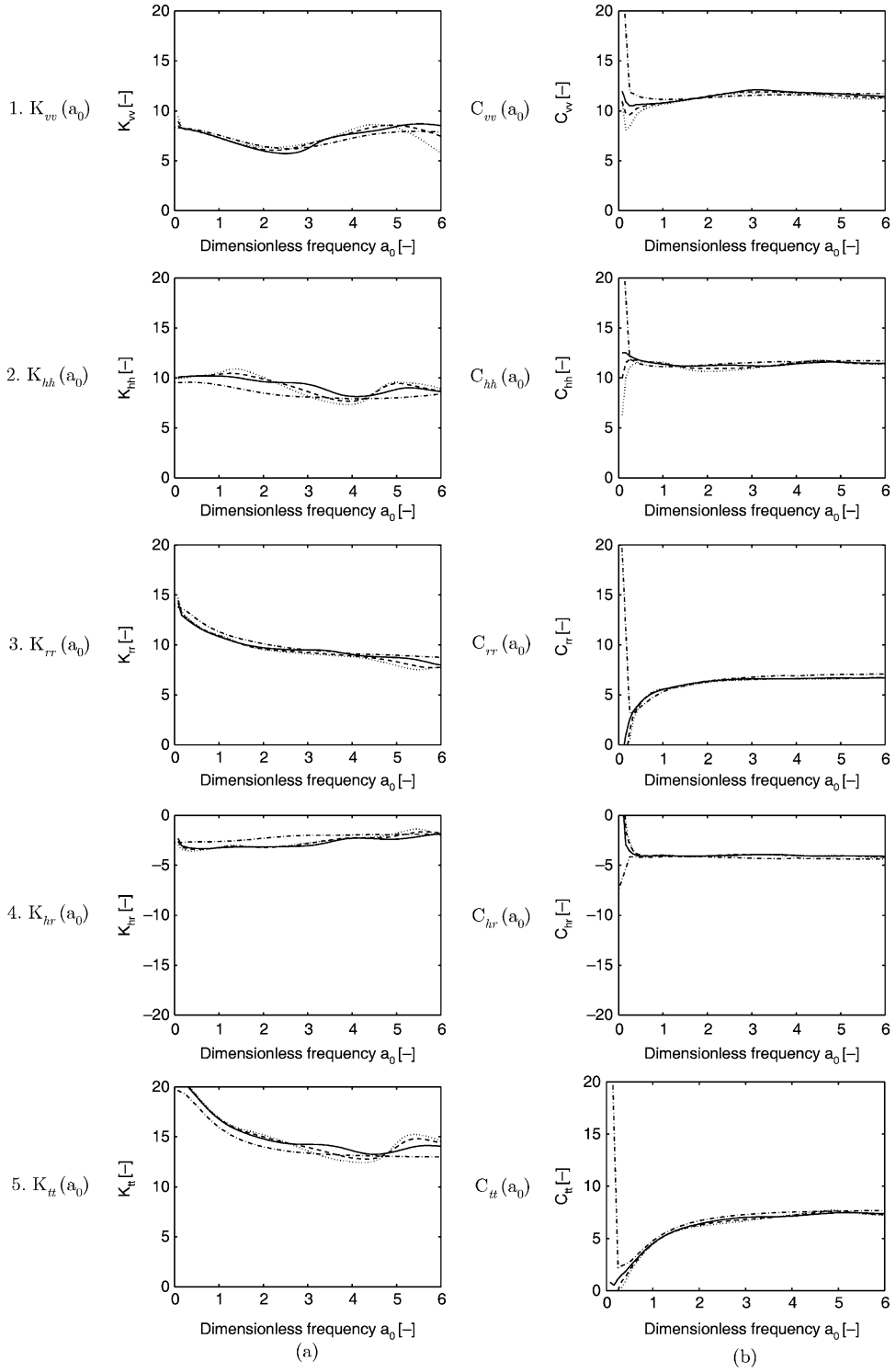

Fig. A.12. (a) Real part $K_{mn}(a_0)$ and (b) imaginary part $C_{mn}(a_0)$ of the dimensionless impedance functions as a function of the dimensionless frequency a_0 for $\bar{h}=1$ and $\bar{\alpha}=i/6$ (solid line), $\bar{\alpha}=i/3$ (dashed line), $\bar{\alpha}=i/2$ (dotted line) and according to Apsel and Luco [37] (dashed-dotted line).

8.7. Choice of the dimensionless distance $\bar{h}$

It has been argued before that the dimensionless distance $\bar{h}$ between the boundaries Σ^- and Σ should be larger than 1 (or that the distance h should be larger than the boundary element size l_e) in order to obtain a good approximation of the derivatives of the displacements and Green's functions. Different values of the dimensionless distance $\bar{h}=1$, $\bar{h}=2$ and $\bar{h}=3$ are therefore considered, while a constant dimensionless coupling parameter $\bar{\alpha}=i/6$ is used.

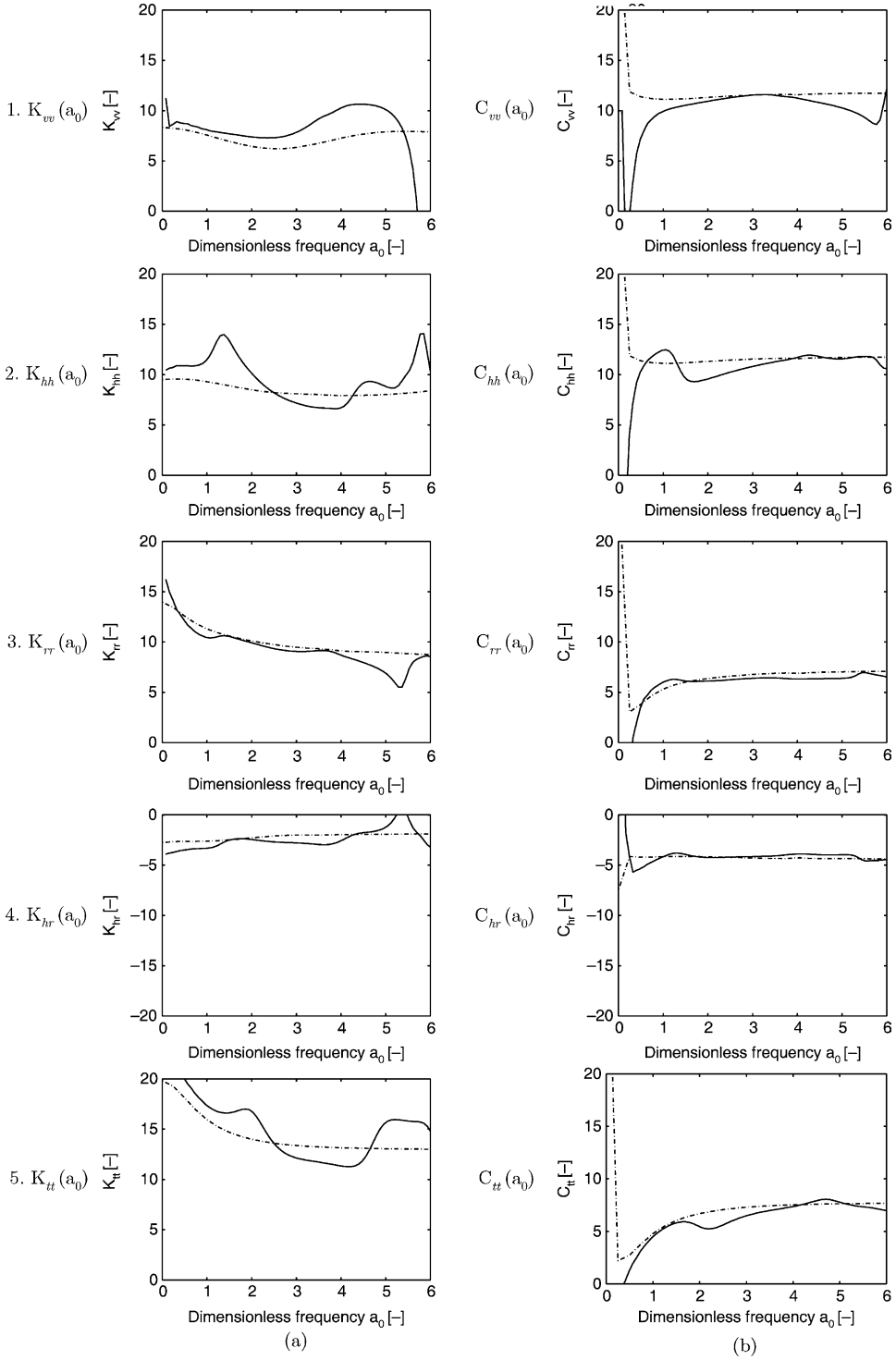

Fig. A.13. (a) Real part $K_{mn}(a_0)$ and (b) imaginary part $C_{mn}(a_0)$ of the dimensionless impedance functions as a function of the dimensionless frequency a_0 for $\bar{h} = 1$ and $\bar{\alpha} = 5i/3$ (solid line) and according to Apsel and Luco [37] (dashed-dotted line).

Fig. A.14a and A.14b shows the real and imaginary part of the dimensionless impedance functions for these three cases. The deviation with the reference results of Apsel and Luco increases for an increasing dimensionless distance $\bar{h}$.

8.8. Recommended values of the dimensionless parameters $\bar{h}$ and $\bar{\alpha}$

The previous parametric study on the impedance functions of a rigid massless cylindrical embedded

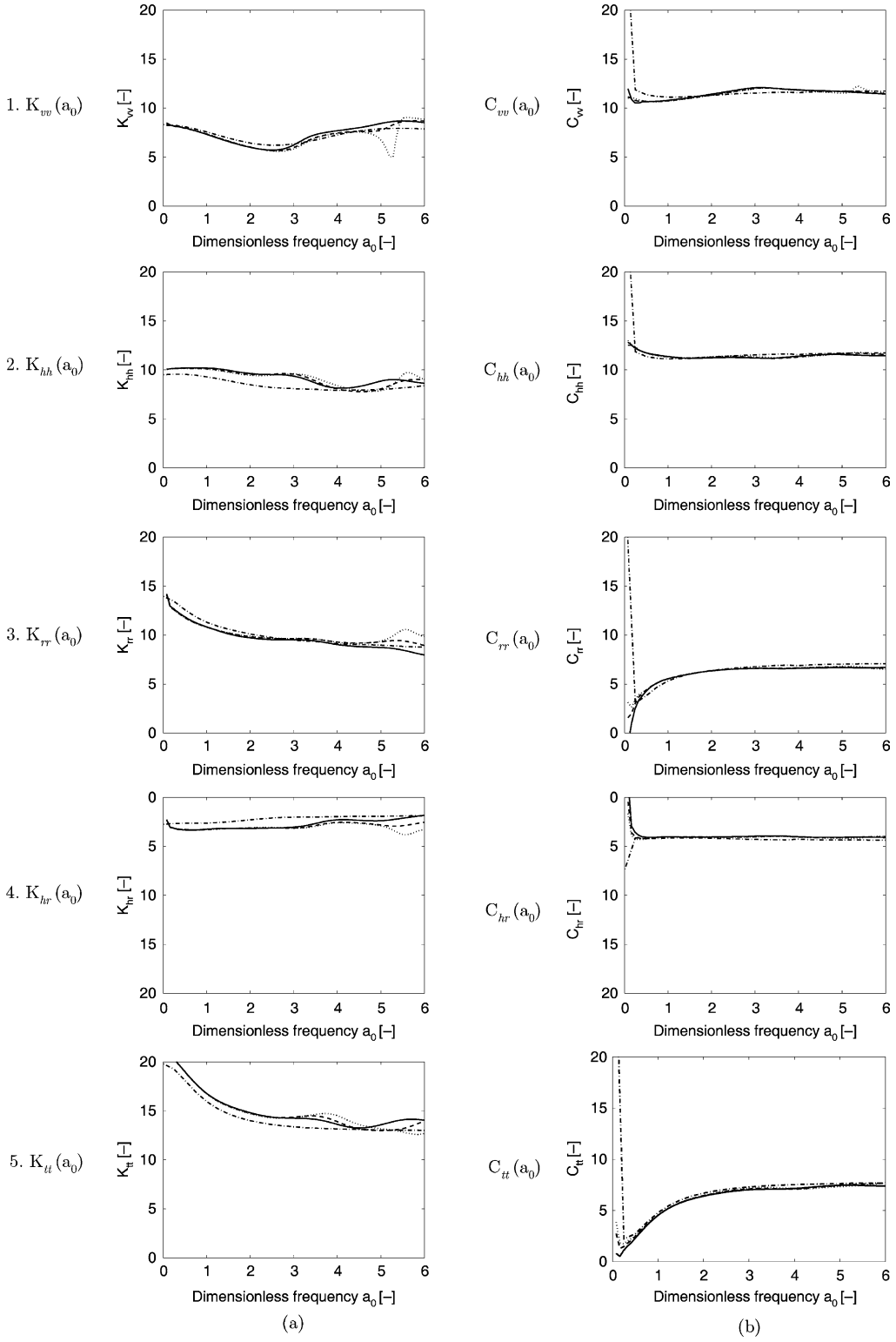

Fig. A.14. (a) Real part $K_{mn}(a_0)$ and (b) imaginary part $C_{mn}(a_0)$ of the dimensionless impedance functions as a function of the dimensionless frequency a_0 for $\bar{\alpha} = i/6$ and $\bar{h} = 1$ (solid line), $\bar{h} = 2$ (dashed line), $\bar{h} = 3$ (dotted line) and according to Apsel and Luco [37] (dashed-dotted line).

foundation has demonstrated that the problem of fictitious eigenfrequencies can be successfully mitigated and that good correspondence with the results of Apsel and Luco is obtained for a dimensionless distance $\bar{h} = 1$ and a constant dimensionless coupling parameter $\bar{\alpha} = i/6$, as illustrated in Fig. A.12.

Fig. A.15 again shows the displacements at the dimensionless frequency $a_0 = 3.33$ in the points located at

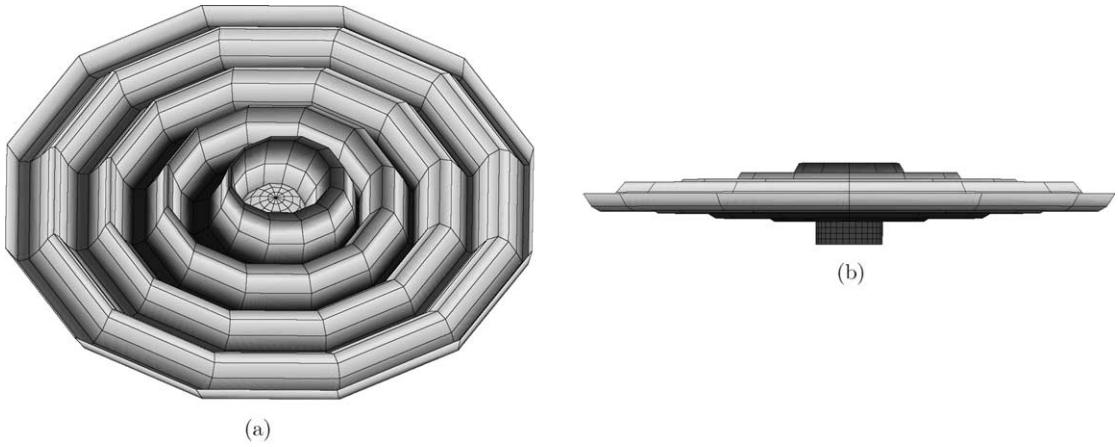

Fig. A.15. (a) Isometric and (b) side view of the displacements of the points on the surface for the rigid massless cylindrical embedded foundation excited by a vertical harmonic point load at a dimensionless frequency $a_0 = 3.33$ and with the parameters $\bar{h} = 1$ and $\bar{\alpha} = i/6$.

the free surface due to a unit vertical harmonic point load applied at the center of the base of the cylindrical foundation. This figure should be compared with results presented earlier in Fig. A.8. The displacements on the free surface of the interior domain Ω_s^{int} are now negligible, which clearly demonstrates that the problem of the fictitious eigenfrequencies has been successfully mitigated.

9. Conclusion

The solution of elastodynamic problems defined on exterior domains with embedded regions of finite extent, using a discretization of a displacement boundary integral equation, is not unique at the eigenfrequencies of the embedded interior domain with Dirichlet boundary conditions along the soil–structure interface and free boundary conditions along the free surface.

The solution technique used in the present paper is derived from the approach proposed by Burton and Miller for acoustic problems. The combination of the boundary integral equation for the displacement and the displacement gradient along the normal direction on the boundary is introduced, using an imaginary coupling parameter α. A modification of this approach, introducing a second parameter h, is proposed to avoid hypersingular terms in the corresponding boundary integral equation. It is proven that fictitious eigenfrequencies are avoided if the parameter h is small enough. The limiting case for h tending to zero has the same properties but requires hypersingular kernels.

Both parameters α and h are written in a dimensionless form and a parametric study is performed on the choice of these parameters, considering the impedance of a rigid massless cylindrical foundation, embedded in a homogeneous halfspace. In the range of dimensionless frequencies up to $a_0^{\max} = 6$, very good correspondence with the results published by Apsel and Luco is obtained with a constant dimensionless coupling parameter $\bar{\alpha} = i/a_0^{\max}$ and a dimensionless distance $\bar{h} = 1$. Spurious non-zero displacements in the interior domain due to fictitious resonances disappear almost completely when these parameters are used. Overestimation of the parameters $\bar{\alpha}$ and $\bar{h}$ or the use of a frequency dependent coupling parameter $\bar{\alpha}$ result in less accurate numerical results.

As the results of this parametric study have proven that the problem of fictitious eigenfrequencies can successfully be mitigated using the combined boundary integral equation, this solution procedure will be used with confidence in the future to compute traffic induced vibrations in buildings with an embedded foundation.

Acknowledgements

The results presented in this paper have been obtained within the frame of the STWW-project IWT000152 'Traffic induced vibrations in buildings'. The financial support of the Ministry of the Flemish Community is gratefully acknowledged.

Appendix A. Proof of uniqueness for the finite difference case

Let Ω be an open bounded domain with a smooth boundary Γ whose unit outward normal vector at the point $\mathbf{x}$ is denoted by $\mathbf{n}$. Since the boundary is smooth, its minimum radius of curvature is greater than r_m. Thus, for any $0 < h < r_m$ the smooth inner surface Γ_h is defined as follows:

$$\Gamma_h = \{\mathbf{x} \in \Omega | \mathbf{x} = \mathbf{x}' - h\mathbf{n};\ \mathbf{x}' \in \Gamma\} \tag{A.1}$$

The part Ω_h of the domain Ω, located between Γ and Γ_h, is mapped as follows:

$$\Omega_h = \{\mathbf{x} \in \Omega | \mathbf{x} = \mathbf{x}' - \zeta h\mathbf{n};\ \mathbf{x}' \in \Gamma;\ \zeta \in]0, 1[\} \tag{A.2}$$

Therefore, the integration of any function $\phi(\mathbf{x})$ over Ω_h can be written as:

$$\int_{\Omega_h} \phi(\mathbf{x})\,\mathrm{d}V(\mathbf{x}) = h\int_{\Gamma}\int_0^1 \phi(\mathbf{x}' - \zeta h\mathbf{n})g(\zeta,\mathbf{x}')\,\mathrm{d}\zeta\,\mathrm{d}S(\mathbf{x}') \quad (A.3)$$

with $g(\zeta, \mathbf{x}') = \mathrm{d}S(\mathbf{x}', \zeta)/\mathrm{d}S(\mathbf{x}')$ tending to 1 if h tends to 0.

It will be demonstrated that there exists a finite h such that the homogeneous elastodynamic problem on Ω has a unique solution that satisfies the following kinematic condition:

$$\mathbf{u}(\mathbf{x}' - h\mathbf{n}) = \left(1 + \frac{h}{\alpha}\right)\mathbf{u}(\mathbf{x}') \quad \forall\,\mathbf{x}' \in \Gamma \quad (A.4)$$

as long a α has a strictly positive imaginary part. This kinematic condition is equivalent to the finite difference form (48) of the mixed boundary condition (44).

This problem is equivalently solved looking for the saddle point of the following Lagrangian $\mathcal{L}(\mathbf{u}, \boldsymbol{\lambda}, \mathbf{w})$:

$$\mathcal{L}(\mathbf{u},\boldsymbol{\lambda},\mathbf{w}) = \frac{1}{2}a(\mathbf{u},\bar{\mathbf{u}}) + \mathrm{Re}\left\{\int_{\Gamma}\boldsymbol{\lambda}(\mathbf{x}')\cdot\left(\mathbf{u}(\mathbf{x}' - h\mathbf{n}) - \left(1+\frac{h}{\alpha}\right)\mathbf{u}(\mathbf{x}')\right)\mathrm{d}S(\mathbf{x}')\right\} + \mathrm{Re}\left\{\int_{\Gamma_h}\mathbf{w}(\mathbf{x})\cdot[\mathbf{t}_n(\mathbf{u})]\,\mathrm{d}S(\mathbf{x})\right\} \quad (A.5)$$

where $\bar{\mathbf{u}}$ is the complex conjugate of $\mathbf{u}$. The standard bilinear form $a(\mathbf{u}, \mathbf{v})$ for elastodynamic problems is defined as:

$$a(\mathbf{u},\mathbf{v}) = \int_{\Omega}(\mathbf{C} : (\mathrm{grad}\,\mathbf{u}\otimes\mathrm{grad}\,\mathbf{v}) - \omega^2\rho\mathbf{u}\cdot\mathbf{v})\,\mathrm{d}V \quad (A.6)$$

with $\mathbf{C}$ the fourth-order elastic tensor. The second term on the right hand side of Eq. (A.5) enforces the kinematic condition (A.4) on the boundary Γ using the Lagrange multipliers $\boldsymbol{\lambda}(\mathbf{x}')$. The third term is added to ensure that no forces are applied on the boundary Γ_h, as is actually the case when the solution is written in terms of single and double layer potentials that are only defined on Γ. The vector $[\mathbf{t}_n(\mathbf{u})]$ denotes the jump of the traction vector $\mathbf{t}_n(\mathbf{u})$ along Γ_h (between Γ_{h+} and Γ_{h-}), while $\mathbf{w}(\mathbf{x})$ is a vector of Lagrange multipliers.

Stating the stationarity of the Lagrangian $\mathcal{L}(\mathbf{u}, \boldsymbol{\lambda}, \mathbf{w})$ with respect to $\mathbf{u}$ gives:

$$-a(\mathbf{u},\mathbf{v}) = \int_{\Gamma_h}(\boldsymbol{\lambda}'(\mathbf{x})\cdot\mathbf{v}(\mathbf{x}) + \mathbf{w}(\mathbf{x})\cdot[\mathbf{t}_n(\mathbf{v})])\,\mathrm{d}S(\mathbf{x}) - \left(1+\frac{h}{\alpha}\right)\int_{\Gamma}\boldsymbol{\lambda}(\mathbf{x}')\mathbf{v}(\mathbf{x}')\,\mathrm{d}S(\mathbf{x}') \quad (A.7)$$

with $\boldsymbol{\lambda}'(\mathbf{x}) = \boldsymbol{\lambda}(\mathbf{x}+h\mathbf{n})/g(1, \mathbf{x}+h\mathbf{n})$. The jump $[\mathbf{t}_n(\mathbf{v})]$ of the traction vector $\mathbf{t}_n(\mathbf{v})$ along Γ_h associated with any field $\mathbf{v}$ defined on Ω is alternatively written as $\mathcal{T}(\mathbf{v})$. If the adjoint operator of $\mathcal{T}(\mathbf{v})$ is denoted as $\mathcal{T}^*(\mathbf{v})$, the line force density $\mathbf{f}_o$ that is applied on Γ_h is defined as $\mathbf{f}_o = -\mathcal{T}^*(\mathbf{w})$. The elastic virtual work on the left hand side of Eq. (A.7) is integrated by parts and the line force density $\mathbf{f}_o$ is introduced, resulting in the following equation:

$$\int_{\Omega}(\mathrm{div}\,\boldsymbol{\sigma}(\mathbf{u}) + \rho\omega^2\mathbf{u})\cdot\mathbf{v}\,\mathrm{d}V = \int_{\Gamma_h}([\mathbf{t}_n(\mathbf{u})] + \boldsymbol{\lambda}' - \mathbf{f}_o)\cdot\mathbf{v}\,\mathrm{d}S + \int_{\Gamma}\left(\mathbf{t}_n(\mathbf{u}) - \left(1+\frac{h}{\alpha}\right)\boldsymbol{\lambda}\right)\cdot\mathbf{v}\,\mathrm{d}S \quad (A.8)$$

This strong formulation enforces the elastodynamic equilibrium equations inside the domain Ω, as well as the following relations between the Lagrange multipliers $\boldsymbol{\lambda}$ and $\mathbf{w}$ and the traction vectors $\mathbf{t}_n(\mathbf{u})$ on Γ and Γ_h:

$$\boldsymbol{\lambda}(\mathbf{x}') = \frac{\alpha}{\alpha+h}\mathbf{t}_n(\mathbf{u})(\mathbf{x}') \quad \mathbf{x}' \in \Gamma \quad (A.9)$$

$$\boldsymbol{\lambda}'(\mathbf{x}) = -[\mathbf{t}_n(\mathbf{u})(\mathbf{x})] + \mathbf{f}_o(\mathbf{x}) \quad \mathbf{x} \in \Gamma_h \quad (A.10)$$

As the jump $[\mathbf{t}_n(\mathbf{u})(\mathbf{x})]$ of the traction vector has to vanish, Eq. (A.10) finally results in $\boldsymbol{\lambda}' = \mathbf{f}_o$.

A main difficulty now occurs when the parameter α in the kinematic condition (A.4) has a non-vanishing imaginary part. In that case, the displacement vector $\mathbf{u}$ may satisfy the kinematic condition on Γ_h, while its conjugate field $\bar{\mathbf{u}}$ does not. This means that the conjugate field $\bar{\mathbf{u}}$ cannot be used as a virtual displacement field $\mathbf{v}$ in Eq. (A.7).

To overcome this drawback, the displacement fields $\mathbf{u}_h$ are defined for any field $\mathbf{u}$ on Ω_h as follows:

$$\mathbf{u}_h(\mathbf{x},\zeta;\mathbf{u}) = (1-\zeta)\beta h\mathbf{u}(\mathbf{x}) \quad \mathbf{x} \in \Gamma_h \quad 0 < \zeta < 1 \quad (A.11)$$

with $\beta = -1/(\alpha + h)$. The functional space V_o is defined as:

$$V_o = \{\mathbf{u}_o \in L_2(\Omega) | \mathrm{grad}\,\mathbf{u}_o \in L_2(\Omega);\ \mathbf{u}_o(\mathbf{x}') = \mathbf{u}_o(\mathbf{x}' - h\mathbf{n}),\ \mathbf{x}' \in \Gamma\} \quad (A.12)$$

The displacement field $\mathbf{u}$ is decomposed as:

$$\mathbf{u} = \mathbf{u}_o + \mathbf{u}_h(\mathbf{u}_o) \quad (A.13)$$

For all $\mathbf{u}_o \in V_o$, the displacement field $\mathbf{u}$ satisfies the kinematic condition (A.4) on Γ since:

$$\left(1+\frac{h}{\alpha}\right)\mathbf{u}(\mathbf{x}') = \left(1+\frac{h}{\alpha}\right)(1+\beta h)\mathbf{u}_o(\mathbf{x}' - h\mathbf{n}) = \mathbf{u}(\mathbf{x}' - h\mathbf{n}) \quad \forall\,\mathbf{x}' \in \Gamma \quad (A.14)$$

The bilinear form $a_o(\mathbf{u}_o, \mathbf{v}_o)$ on V_o is now defined as:

$$a_o(\mathbf{u}_o, \mathbf{v}_o) = a(\mathbf{u}_o + \mathbf{u}_h(\mathbf{u}_o), \bar{\mathbf{v}}_o + \mathbf{u}_h(\bar{\mathbf{v}}_o)) - \int_{\Gamma_h} \mathbf{f}_o \cdot \bar{\mathbf{v}}_o \, \mathrm{d}S \tag{A.15}$$

Eqs. (A.9) and (A.10) allow to elaborate this definition as:

$$a_o(\mathbf{u}_o, \mathbf{v}_o) = a(\mathbf{u}_o + \mathbf{u}_h(\mathbf{u}_o), \bar{\mathbf{v}}_o + \mathbf{u}_h(\bar{\mathbf{v}}_o)) - (1 + \beta h) \int_{\Gamma} \mathbf{t}_n(\mathbf{u}_o + \mathbf{u}_h(\mathbf{u}_o)) \cdot \bar{\mathbf{v}}_o \, \mathrm{d}S \tag{A.16}$$

When it is understood that the displacement field $\mathbf{v} = \mathbf{v}_o + \mathbf{u}_h(\mathbf{v}_o)$ satisfies the kinematic condition (A.4), the definitions (A.15) and (A.16) are equivalent to Eq. (A.7) as the terms in the Lagrange multipliers $\boldsymbol{\lambda}(\mathbf{x}')$ and $\boldsymbol{\lambda}'(\mathbf{x})$ do not contribute to the work. A solution $\mathbf{u}$ of the elastodynamic problem on Ω with the kinematic condition (A.4) has to satisfy:

$$a_o(\mathbf{u}_o, \mathbf{v}_o) = 0 \quad \forall \, \mathbf{v}_o \in V_o \tag{A.17}$$

In particular, the following imaginary part must be equal to zero:

$$\mathrm{Im}(a_o(\mathbf{u}_o, \mathbf{u}_o)) = 0 \tag{A.18}$$

Noticing that $\mathbf{u}_h(\mathbf{u}) = (\beta_r + i\beta_i) h \mathcal{H} \mathbf{u}$, with $\mathcal{H} = (1 - \zeta)\gamma_h$ a real operator that is built from the trace operator γ_h on Γ_h, it can be shown that:

$$\mathrm{Im}(a_o(\mathbf{u}_o, \mathbf{u}_o)) = 2h\beta_i (h\beta_r a_h(\mathcal{H}\mathbf{u}_o, \mathcal{H}\bar{\mathbf{u}}_o) + a_h(\mathcal{H}\mathbf{u}_{or}, \mathbf{u}_{or}) + a_h(\mathcal{H}\mathbf{u}_{oi}, \mathbf{u}_{oi})) - \mathrm{Im}\left((1 + \beta h) \int_{\Gamma} \mathbf{t}_n(\mathbf{u}_o + \mathbf{u}_h(\mathbf{u}_o)) \cdot \bar{\mathbf{v}}_o \, \mathrm{d}S \right) \tag{A.19}$$

where $a_h(\mathbf{u},\mathbf{v})$ denotes the same bilinear form as $a(\mathbf{u},\mathbf{v})$, except that the integral is performed only on the domain Ω_h, as $\mathbf{u}_h(\mathbf{u}_o)$ vanishes elsewhere. The stresses $\mathbf{t}_n(\mathbf{u}_o)$ and $\mathbf{t}_n(\mathbf{u}_h(\mathbf{u}_o))$ in Eq. (A.19) are elaborated using the constitutive equations and the following expressions for the gradients of the displacement fields:

$$\mathrm{grad}\, \mathbf{u} = \frac{1}{h} \mathbf{n} \otimes \partial_{\zeta} \mathbf{u} + \mathrm{grad}_h \mathbf{u} \tag{A.20}$$

$$\mathrm{grad}\, \mathcal{H}\mathbf{u} = \frac{1}{h} \mathbf{n} \otimes \gamma_h \mathbf{u} + (1 - \zeta) \mathrm{grad}_h \gamma_h \mathbf{u} \tag{A.21}$$

where grad_h is the gradient in the plane normal to $\mathbf{n}$. Integrating with respect to ζ when possible, accounting for $\mathbf{u}_o(\mathbf{x}) = \mathbf{u}_o(\mathbf{x} + h\mathbf{n})$ when $\mathbf{x} \in \Gamma_h$ and sorting all terms with respect to powers of h, it can be demonstrated that only the last term of Eq. (A.19) gives a contribution in h^0, while the other terms are at least $\mathrm{O}(h)$, so that:

$$\mathrm{Im}(a_o(\mathbf{u}_o, \mathbf{u}_o)) = \mathrm{Im}\left(\int_{\Gamma} \mathbf{Q} : (\partial_{\mathbf{n}} \mathbf{u}_o \otimes \bar{\mathbf{u}}_o) \, \mathrm{d}S \right) + \beta_i \|\mathbf{u}_o\|_Q^2 + \mathrm{O}(h) \tag{A.22}$$

In this equation, $\|\mathbf{u}_o\|_Q^2$ is defined as:

$$\|\mathbf{u}_o\|_Q^2 = \int_{\Gamma} \mathbf{Q} : (\mathbf{u} \otimes \bar{\mathbf{u}}) \, \mathrm{d}S \tag{A.23}$$

with $\mathbf{Q}$ the acoustic tensor defined as $Q_{il}(\mathbf{x}) = C_{ijkl} n_j n_k$. Since the acoustic tensor is positive definite, $\|\mathbf{u}_o\|_Q^2$ is equivalent to the L_2-norm $\|\mathbf{u}_o\|_{\Gamma}^2$ on Γ.

Before going further, it is worth to look at the asymptotic solution when h tends to zero. Inside the domain Ω_h, $\mathbf{u}_h$ dominates; more precisely, $\beta \mathbf{n} \otimes \gamma_h \mathbf{u}$ dominates the gradient which is constant when ζ varies. Therefore, the traction vectors $\mathbf{t}_n(\mathbf{u})$ on the two sides of Ω_h are equal. As $[\mathbf{t}_n(\mathbf{u})] = 0$, they are also equal to the traction vector on the other side of Γ_h:

$$\mathbf{t}_n(\mathbf{u})(\mathbf{x}) = \mathbf{t}_n(\mathbf{u})(\mathbf{x}' - h^{\pm}\mathbf{n}) = \beta \mathbf{Q} \mathbf{u}(\mathbf{x}' - h\mathbf{n}) \quad \mathbf{x}' \in \Gamma \tag{A.24}$$

In order to obtain a well-posed limit problem, the following is stated:

$$\lim_{h \to 0} \mathbf{t}_n(\mathbf{u})(\mathbf{x}) = i\xi \mathbf{Q} \mathbf{u}(\mathbf{x}') \tag{A.25}$$

which can be easily achieved by taking $\alpha = i/\xi$. As for a smooth boundary, any solution of the homogeneous elastodynamic equation on Ω_h for $\omega \leq \omega_0$ is continuous and has continuous derivatives up to any order inside Ω_h, all fields including $\mathrm{grad}_h \mathbf{u}_o$ and $\partial_{\mathrm{nn}}^2 \mathbf{u}_o$ can be bounded independently from h, provided that the limit when h tends to zero is well defined. Using a Taylor expansion along the normal for $\mathbf{u}_o$ up to the second-order and noticing that $\mathbf{u}_o(\mathbf{x} - h\mathbf{n}) = \mathbf{u}_o(\mathbf{x})$ for $\mathbf{x} \in \Gamma$ one can show that $\partial_{\mathbf{n}} \mathbf{u}_o = \mathrm{O}(h)$ on Γ. Thus, if $\|\mathbf{u}_o\|_{\Gamma_h}^2 \geq A > 0$ for $h \leq h_o$, there exists a real number c so that the following inequality holds $\forall h \leq h_o$ and $\forall \omega \leq \omega_o$:

$$\left| \mathrm{Im}(a_o(\mathbf{u}_o, \mathbf{u}_o)) - \beta_i \|\mathbf{u}_o\|_Q^2 \right| \leq ch \|\mathbf{u}_o\|_{\Gamma}^2 \tag{A.26}$$

As the imaginary part of β is strictly positive, $\beta_i \geq \xi > 0$, and the following inequality must also hold:

$$\mathrm{Im}(a_o(\mathbf{u}_o, \mathbf{u}_o)) \geq c' \xi \|\mathbf{u}_o\|_{\Gamma}^2 \tag{A.27}$$

uniformly in h with c' a positive real number. As the imaginary part $\mathrm{Im}(a_o(\mathbf{u}_o,\mathbf{u}_o))$ must be equal to zero according to Eq. (A.18), the inequality (A.27) implies that $\|\mathbf{u}_o\|_{\Gamma}^2 = 0$, resulting in $\mathbf{u} = 0$ on Γ and on Γ_h.

For an excitation frequency ω that is lower than the first eigenfrequency of Ω_h with clamped boundary conditions on Γ_h and Γ, it is known that the unique elastodynamic solution without body forces corresponds to $\mathbf{u}_o = 0$ everywhere

inside Ω_h. Consequently, $\mathbf{t}_n(\mathbf{u}_0)=0$ and $\boldsymbol{\lambda}=0$. As the only elastodynamic solution on a bounded domain that satisfies $\mathbf{u}=0$ and $\mathbf{t}_n(\mathbf{u})=0$ on its boundary corresponds to $\mathbf{u}=0$ everywhere inside this domain, it can be concluded that $\mathbf{u}_o=0$ everywhere inside Ω. The uniqueness of the inner problem with the kinematic condition (A.4) is then proven for $h<h_o$ and $\omega<\omega_o$, including the limiting case when h tends to zero. In the latter case, the kinematic condition (A.4) corresponds to the following condition:

$$\mathbf{u} + \alpha\partial_n\mathbf{u} = 0 \tag{A.28}$$

References

[1] Aubry D, Clouteau D. A subdomain approach to dynamic soil–structure interaction. In: Davidovici V, Clough RW, editors. Recent advances in earthquake engineering and structural dynamics. Ouest Editions. Nantes: AFPS; 1992, p. 251–72.

[2] Clouteau D. Propagation d'ondes dans des milieux hétérogènes. Application à la tenue des ouvrages sous séismes. PhD thesis, Laboratoire de Mécanique des Sols, Structures et Matériaux, Ecole Centrale de Paris; 1990.

[3] Kausel E, Roësset JM. Stiffness matrices for layered soils. Bull Seismol Soc Am 1981;71(6):1743–61.

[4] Luco JE, Apsel RJ. On the Green's functions for a layered half-space. Part I. Bull Seismol Soc Am 1983;4:909–29.

[5] Apsel RJ, Luco JE. On the Green's functions for a layered half-space. Part II. Bull Seismol Soc Am 1983;73:931–51.

[6] Degrande G, De Roeck G, Van den Broeck P, Smeulders D. Wave propagation in layered dry, saturated and unsaturated poroelastic media. Int J Solids Struct 1998;35(34/35):4753–78. Poroelasticity Maurice A. Biot memorial issue.

[7] Guzina BB, Pak RYS. On the analysis of wave motions in a multi-layered solid. Quart J Mech Appl Math 2001;54(1):13–37.

[8] Bonnet M. Boundary integral equation methods for solids and fluids. England: Wiley; 1995.

[9] Dominguez J. Boundary elements in dynamics. Co-published by Computational Mechanics Publications, Southampton, Boston and Elsevier Applied Science London, New York; 1993.

[10] Pyl L, Degrande G. Numerical modeling of traffic induced vibrations in buildings using a dynamic soil–structure interaction analysis. Report BWM-2002-11, Department of Civil Engineering, K.U. Leuven; December 2002.

[11] Copley LG. Integral equation method for radiation from vibrating bodies. J Acoust Soc Am 1967;41:807–16.

[12] Schenck HA. Improved integral formulation for acoustic radiation problems. J Acoust Soc Am 1968;44:45–58.

[13] Piaszczyk CM, Klosner JM. Acoustic radiation from vibrating surfaces at characteristic frequencies. J Acoust Soc Am 1984;75(2): 363–75.

[14] Burton AJ, Miller GF. The application of integral equation methods to the numerical solution of some exterior boundary-value problems. Proc R Soc Lond 1971;323:201–10.

[15] Amini S. On the choice of the coupling parameter in boundary integral formulations of the exterior acoustic problem. Applic Anal 1990;35: 75–92.

[16] Chen JT, Chen KH, Chen CT. Adaptive boundary element method of time-harmonic exterior acoustics in two dimensions. Comput Meth Appl Mech Eng 2002;191:3331–45.

[17] Chen JT, Chen KH, Chen IL, Liu LW. A new concept of modal participation factor for numerical instability in the dual bem for exterior acoustics. Mech Res Commun 2003;30:161–74.

[18] Ursell F. On the exterior problems of acoustics. Proc Cambridge Philos Soc 1973;74:117–25.

[19] Jones DS. Integral equations for the exterior acoustic problem. Quart J Mech Appl Math 1974;27:129–42.

[20] Brod K. On the uniqueness of solution for all wavenumbers in acoustic radiation. J Acoust Soc Am 1984;76(4):1238–43.

[21] Kobayashi S, Nishimura N. On the indeterminancy of BIE solutions for the exterior problems of time-harmonic elastodynamics and incompressible elastostatics. In: Brebbia CA, editor. Boundary element methods in engineering. Berlin: Springer; 1982, p. 282–96.

[22] Kobayashi S, Nishimura N. Dynamic analysis of underground structures by the integral equation method. In: Eisenstein Z, editor. Numerical methods in geomechanics. Rotterdam: A.A. Balkema; 1982, p. 401–9.

[23] Kobayashi S, Nishimura N. Transient stress analysis of tunnels and cavities of arbitrary shape due to travelling waves. In: Banerjee PK, Shaw RP, editors. Developments in boundary element methods, vol. 2. London: Applied Science Publishers; 1982, p. 177–210.

[24] Gonsalves IR, Shippy DJ, Rizzo FJ. The direct boundary integral-equation method for the 3-dimensional elastodynamic transmission problem. Math Comput Model 1991;15(1–3):155–64.

[25] Jones DS. Boundary integrals in elastodynamics. IMA J Appl Math 1985;34:83–97.

[26] Liu YJ, Rizzo FJ. Hypersingular boundary integral-equations for radiation and scattering of elastic waves in 3 dimensions elastodynamic transmission problem. Comput Meth Appl Mech Eng 1993; 107(1–2):131–44.

[27] Eringen AC, Suhubi ES. Elastodynamics. Linear theory, vol. 2. New York, USA: Academic Press; 1975.

[28] Aubry D, Clouteau D. A regularized boundary element method for stratified media. In: Cohen G, Halpern L, Joly P, editors. Proceedings of the first international conference on mathematical and numerical aspects of wave propagation phenomena, Strasbourg, France. Philadelphia, PA: SIAM; April 1991, p. 660–8.

[29] Rizzo FJ, Shippy DJ, Rezayat M. A boundary integral equation method for radiation and scattering. Int J Numer Meth Eng 1985;21: 115–29.

[30] Bui HD, Loret B, Bonnet M. Régularisation des équations intégrales de l'élastodynamique et de l'élastostatique. Compte Rendu à l' Académie des Sciences: série II 1985;t.300(14):633–6.

[31] Bonnet M. Méthode des équations intégrales régularisées en élastodynamique. PhD thesis, Ecole Nationale des Ponts et Chaussées; 1986.

[32] Hall WS, Oliveto G. Boundary element methods for soil–structure interaction. Dordrecht: Kluwer Academic Publishers; 2003.

[33] Guzina BB, Pak RYS. Static fundamental solutions for a bi-material full-space. Int J Solids Struct 1999;36:493–516.

[34] Blanchet L, Faye G. Hadamard regularization. J Math Phys 2000; 41(11):7675–714.

[35] Becache E, Nedelec JC, Nishimura N. Regularization in 3d for anisotropic elastodynamic crack and obstacle problems. J Elast 1993; 31:25–46.

[36] Beskos DE. Mechanics and mathematical methods. First series: computational methods in mechanics. Vol. 3: Boundary element methods in mechanics. Amsterdam, The Netherlands: Elsevier Science Publishers; 1987.

[37] Apsel RJ, Luco JE. Impedance functions for foundations embedded in a layered medium: an integral equation approach. Earthquake Eng Struct Dyn 1987;15:213–31.

[38] Sieffert J.-G., Cevaer F. Handbook of impedance functions. Surface foundations, Ouest Editions. Nantes: Presses Académiques; 1992.

[39] Kennett BLN. Seismic wave propagation in stratified media. Cambridge: Cambridge University Press; 1983.